

EMERGENCY DEPARTMENT PATIENT FLOW OPTIMIZATION WITH AN ALTERNATIVE CARE THRESHOLD POLICY

SAHBA BANIASADI, PAUL M. GRIFFIN, AND PRAKASH CHAKRABORTY

ABSTRACT. Emergency department (ED) overcrowding and patient boarding represent critical systemic challenges that compromise care quality. We propose a threshold-based admission policy that redirects non-urgent patients to alternative care pathways, such as telemedicine, during peak congestion. The ED is modeled as a two-class $M/M/c$ preemptive-priority queuing system, where high-acuity patients are prioritized and low-acuity patients are subject to state-dependent redirection. Analyzed via a level-dependent Quasi-Birth-Death (QBD) process, the model determines the optimal threshold by maximizing a long-run time-averaged objective function comprising redirection-affected revenue and costs associated with patient balking and system occupancy. Numerical analysis using national healthcare data reveals that optimal policies are highly context-dependent. While rural EDs generally optimize at lower redirection thresholds, urban EDs exhibit performance peaks at moderate thresholds. Results indicate that our optimal policy yields significant performance gains of up to 4.84% in rural settings and 5.90% in urban environments. This research provides a mathematically rigorous framework for balancing clinical priority with operational efficiency across diverse ED settings.

1. INTRODUCTION

The overcrowding of emergency departments (EDs) in the United States (US) is a persistent and complex problem driven by a range of systemic problems. One major contributor is the limited availability of inpatient beds, which delays the transfer of patients from the ED to hospital units, a process known as "boarding". This results in longer wait times for incoming patients, reduced capacity to treat emergencies, and increased stress on medical staff (Powell et al., 2012; Kennedy et al., 2025). Additionally, EDs often serve as a safety net for uninsured or under-insured individuals who may lack access to primary care, leading to a surge in non-urgent visits that further strain resources (Cowling and Majeed, 2013; Yun et al., 2025). The mismatch between patient demand and hospital capacity can lead to inefficient care delivery and compromised patient outcomes (Jones et al., 2022; Nyce et al., 2021).

Another key challenge is the shortage of healthcare personnel, particularly nurses and emergency physicians, which leads to burnout (Phillips et al., 2022). Limited staffing makes it difficult to meet the needs of a high-volume patient population, especially during peak hours or public health crises. Overcrowding also negatively affects clinical workflows, increasing the risk of medical errors, patient dissatisfaction, and overall healthcare costs. Addressing ED overcrowding requires coordinated policy interventions such as investment in primary care access, streamlined care coordination, improved

MARCUS DEPARTMENT OF INDUSTRIAL AND MANUFACTURING ENGINEERING, THE PENNSYLVANIA STATE UNIVERSITY

E-mail address: sqb6360@psu.edu, pmg14@psu.edu, and prakashc@psu.edu.

discharge planning, and expanded community-based alternatives to emergency care (Sartini et al., 2022).

When demand for emergency services exceeds available resources, system congestion drives longer wait times, increased rates of patients leaving without being seen (LWBS), ambulance diversion, diminished patient satisfaction, and worse clinical outcomes. According to the American College of Emergency Physicians, overcrowding is defined as "a situation that occurs when the identified need for emergency services exceeds available resources for patient care in ED, hospital, or both" (Savioli et al., 2022; American College of Emergency Physicians Task Force on Boarding, 2008).

From an operations and systems perspective, overcrowding reflects a fundamental imbalance between stochastic demand and finite, heterogeneous service capacity, compounded by priority-based clinical decision rules and limited routing flexibility. This makes emergency departments a natural application domain for queuing-theoretic and control-based models that can support real-time operational policies under uncertainty.

Various approaches have been developed to address ED overcrowding. These include assigning physicians or advance-practice clinicians to triage to assist in evaluation and initiate treatment, "fast-tracking" low-severity patients (e.g., minor injuries, sore throats) to a separate area that doesn't use ED beds for treatment, offering remote assessment such as telehealth to low-acuity patients, using a flow coordinator to facilitate patient flow, and steering patients that don't require ED care to other settings. While these interventions have demonstrated measurable benefits, they are often implemented as static structural changes rather than as dynamic, state-dependent operational policies that respond to real-time congestion levels. This limits their ability to adapt to transient surges in demand, staffing fluctuations, or seasonal variability in patient mix.

We propose a threshold-based admission policy to address ED overcrowding that offers an alternative service to non-severe patients when the system occupancy exceeds a specific threshold. For this case, patients have been assessed at triage into severe and non-severe categories and offered the alternative once the assessment is completed. The alternative service depends on the type of setting and could include telemedicine in rural settings and affiliated clinics for hospital networks in urban settings.

The key contribution of this work is to formalize this operational intuition as an analytically tractable, threshold-based control policy embedded within a multi-class stochastic service system. We model the ED as a two-class $M/M/c$ preemptive-priority queuing system analyzed via a level-dependent Quasi-Birth-Death (QBD) process. This framework considers both revenue and costs (e.g., waiting and balking costs) to determine the optimal threshold by maximizing a long-run time-averaged objective function. The approach is applied across a variety of hospital settings including rural and urban-based hospitals to quantify the potential benefit by setting. Our numerical results indicate that this optimal policy yields significant performance gains of up to 4.84% in rural settings and 5.90% in urban environments. Unlike prior work that focuses primarily on performance metrics such as waiting time or length of stay, our model explicitly integrates financial, operational, and behavioral components into a unified long-run objective function. This allows hospital decision-makers to evaluate not only clinical flow improvements, but also the economic and access-related implications of redirecting non-urgent demand.

The layout of this paper is as follows. In Section 2, we present a review of the literature on improving ED overcrowding and multi-class queuing systems with preemption. The detailed problem description is provided in Section 3 followed by the model description in Section 4. Methods for determining the steady state distribution, validation of the approach, and implementation of the objective function components are discussed in Section 5. Results and sensitivity analysis are presented in Section 6 for a variety of hospital settings. Conclusions and future work are discussed in Section 7.

2. LITERATURE REVIEW

This section reviews two key areas that shape the work presented in the paper. This includes a discussion of operational interventions to address ED overcrowding followed by a discussion of queuing-based methods suitable for priority-based patient flow.

2.1. Approaches for Reducing ED Overcrowding. Overcrowding in the ED stems from an imbalance between hospital capacity and demand for services, and has been identified as a primary barrier to providing safe and efficient patient care (Morley et al., 2018; Savioli et al., 2022). In addition to expanding physical capacity, interventions fall into three main categories: i) input-level interventions, ii) throughput-level interventions, and iii) output-level interventions.

Input-level interventions focus on improving the triage process and reducing non-urgent arrivals. Assigning a physician or an advanced-practice clinician to triage can streamline decision-making and initiate treatment earlier. In a case-controlled study Han et al. (2010) found that physician-based triage decreased LWBS rates but had only a modest effect of patient ED waiting times to be seen (WT) and length of stay (LOS) times. However, a meta-analysis of 30 studies on the impact of physician-based triage on ED LOS found that median time decreased by 15.3 minutes compared to traditional nurse led triage (Jeyaraman et al., 2022). Kamali et al. (2019) developed a steady-state, many-server fluid approximation to show that physician-based triage can outperform nurse-based triage when arrival rates are high. Zayas-Caban et al. (2019) modeled triage and treatment as a two-stage stochastic system developing a heuristic-based threshold to prioritize triage versus treatment for low-acuity patients.

Reducing non-urgent arrivals can also be achieved by introducing an alternative service such as telemedicine. Two systematic reviews (Tsou et al., 2021; Scott et al., 2025) showed that in rural areas this approach can help reduce ED WT and LOS without compromising patient outcomes. Using a large data set from New York state, Sun et al. (2020) also found that telemedicine in the ED significantly reduces LOS.

Throughput-level interventions focus on improving flow within the ED. One approach is "fast-tracking" low-acuity patients (based on the emergency severity index (ESI)) to a dedicated area that does not utilize ED beds. Several studies show this reduces overall WT and LOS without negatively impacting high-acuity patients (Considine et al., 2008; Chrusciel et al., 2019). However, Ferrand et al. (2018) used simulation to compare fast-track to a dynamic priority queue (DPQ) approach, which prioritizes patients based on ESI and accumulated wait times. In their model, DPQ dominated fast-track in several performance measures. Other studies have also supported the use of DPQ (Hou and Zhao, 2020; Alipour-Vaezi et al., 2022).

Additionally, point of care (POC) testing and diagnostics (Fermann and Suyama, 2002). (e.g., portable molecular PCR platforms for rapid pathogen detection, troponin assays for early detection of myocardial infarction, and connected devices for rapid ECG, images, or other vitals) can help reduce ED WT (Rooney and Schilling, 2014).

Further throughput gains have been realized by organizing personnel into dedicated care teams. A team-based assignment system (one physician, two nurses, one technician) implemented at a suburban ED resulted in significant reductions in both patient waiting times and LWBS rates (Patel and Vinson, 2005), while also enhancing patient satisfaction (DeBehnke and Decker, 2002).

Output-level interventions address the efficient disposition of patients, specifically focusing on the "boarding" phenomenon where admitted patients await transfer to inpatient beds. Boarding diminishes ED capacity and is a critical determinant of ambulance diversion (Asplin et al., 2003). The detrimental effects are substantial; research demonstrates a dose-dependent association between ED stays exceeding five hours and increased 30-day mortality, with standardized mortality ratios rising by 10% for patients boarding 8-12 hours (Jones et al., 2022).

Improving inpatient bed availability through enhanced discharge planning is a primary mitigation strategy. Computer modeling has demonstrated that hospitals achieving 75% of inpatient discharges by noon reduced ED boarding hours from 77.0 to 3.0 hours daily, while shifting peak discharge times four hours earlier could eliminate boarding entirely (Powell et al., 2012). This analysis revealed that synchronizing inpatient discharge patterns with periods of peak ED demand for beds can substantially decrease the duration admitted patients spend awaiting transfer from the emergency department.

2.2. Applicable Multi-Class queuing Models. An ED can be modeled as a stochastic service system characterized by unscheduled arrivals, finite service capacity determined by beds and clinical staff, heterogeneity in patient acuity, and real-time decisions regarding routing, prioritization, and redirection. These structural features naturally align with multi-class queuing models, particularly those incorporating priority mechanisms.

The methodological foundation for analyzing block-structured stochastic systems lies in the matrix geometric methods pioneered by Neuts (1994) and further systematized by Latouche and Ramaswami (1999). Building upon this general theory, a foundational framework for priority-based multi-class queues was established by Kao and Narayanan (1991), who analyzed a multiprocessor system with preemptive priorities and introduced a tractable method for computing steady-state distributions. We utilize their specific formulation because it explicitly captures the complex level-dependent transitions inherent in multi-server systems with preemption, which are not easily tractable via standard birth-death approximations. Although motivated by computer-processing environments, the underlying mechanics are directly applicable to ED operations, where high-acuity (urgent) patients preempt service for lower-acuity individuals. Crucially, this approach allows for the exact calculation of steady-state probabilities in systems with complex, level-dependent transitions that are difficult to analyze via standard birth-death processes.

Subsequent research has adapted such priority-driven frameworks to healthcare settings. Stochastic population models for ED crowding show how time-varying arrival rates, length-of-stay dynamics, and capacity constraints collectively shape fluctuations in ED occupancy and crowding

levels (Parnass et al., 2023). Although not explicitly formulated as multi-class queues, these models capture key sources of heterogeneity.

The importance of class-based competition for scarce ED resources is also reflected in the broader patient-flow and scheduling literature. A review of queuing and optimization models, (Saghafian et al., 2015), highlights how acuity differences and resource needs shape operational performance. Beyond the ED, multi-class queuing formulations have examined routing and staffing across networks. For example, a multiclass–multiserver model with workload-dependent service times showed that variability in workload and class-dependent priorities significantly affect system delays (Nambiar et al., 2023).

Queuing theory has also shaped dynamic routing and admission-control policies, often modeled by Markov decision processes (MDPs). While Markov Decision Processes (MDPs) are often used to derive optimal routing policies, they can suffer from the "curse of dimensionality" in large state spaces. In contrast, our work utilizes the structural properties of threshold-based policies to formulate a tractable QBD process.

In summary, the literature demonstrates that multi-class queuing systems incorporating priority, preemption, and dynamic routing provide a rigorous analytical foundation for modeling ED operations. The methodological insights from matrix-analytic frameworks for priority-based queues (Kao and Narayanan, 1991), combined with ED-specific queuing and patient-flow models (Parnass et al., 2023; Saghafian et al., 2015; Nambiar et al., 2023), motivate the formulation of our preemptive-priority queue with a threshold-based redirection mechanism for non-urgent patients.

3. MODEL DESCRIPTION AND PROBLEM FORMULATION

3.1. System Overview and Control Objective. We address ED congestion by identifying an optimal threshold policy for offering alternative care (such as telemedicine or affiliated urgent care clinics) to non-urgent patients when system demand is high. The objective is to maximize revenue penalized by waiting and balking costs. We model the ED as a two-class $M/M/c$ priority queuing system with distinct service time distributions for urgent and non-urgent patients. This framework is designed to provide hospital administrators with an implementable decision tool for efficient ED management.

Patient Flow and Priority Structure. Patients arrive either via ambulance or as walk-ins and are triaged into *urgent* (ambulance arrivals and walk-in triage levels 1-2) or *non-urgent* (triage levels 3-5) classes. Urgent patients are prioritized for immediate service, while non-urgent patients are assigned lower priority. Non-urgent patients may either enter the ED queue or be offered an external alternative-care option depending on a congestion threshold. This mechanism optimizes resource allocation by directing lower-acuity patients to suitable external or lower-intensity care pathways. The ED is thus modeled as a two-class preemptive-priority $M/M/c$ system with state-dependent threshold-based admission of non-urgent arrivals.

Alternative Care. In this study, alternative care refers to any lower-acuity treatment pathway available to non-urgent patients outside the main emergency department. These options may include telemedicine consultations, affiliated urgent care clinics, or hospital-based outpatient services that

can deliver appropriate treatment at a lower operational cost and shorter wait time. From a modeling perspective, the alternative care pathway is associated with its own revenue rate (e.g. r^{Alt} for in-person alternatives or r^{Tele} for telemedicine) and potential balking or acceptance costs. The acceptance probability p_a denotes the probability that a non-urgent patient accepts the offered alternative care option, regardless of its specific form.

3.2. Queuing Model with Threshold-based Admission and Balking. We now explain in detail our model of the ED as a two-class $M/M/c$ priority queuing system. We assume all patients arrive according to a Poisson process at a total rate λ . Furthermore, *urgent* patients arrive with probability p_u , and *non-urgent* patients with probability $p_n = 1 - p_u$. This yields effective arrival rates $\lambda_u = \lambda p_u$ for urgent patients and $\lambda_n = \lambda p_n$ for non-urgent patients, each with exponentially distributed service times at rates μ_u and μ_n , respectively.

The total number of patients in the system at time t is $N(t) = N_u(t) + N_n(t)$, where $N_u(t)$ and $N_n(t)$ denote the numbers of urgent and non-urgent patients, respectively. When $N(t)$ reaches or exceeds a balking threshold k , newly arriving non-urgent patients *balk*, that is, leave without entering the system. If $N(t) < k$ non-urgent arrivals enter the system. However, when the system occupancy lies between a lower threshold θ and k , non-urgent arrivals may be routed to alternative care with probability p_a . Formally:

- (i) If $\theta \leq N(t) < k$, an incoming non-urgent patient is offered alternative care. This offer is accepted with probability p_a or declined with probability $(1 - p_a)$. Patients who decline the offer remain in the ED for treatment.
- (ii) If $N(t) < \theta$, a non-urgent patient stays in the ED for treatment.

The ED is equipped with c_u urgent beds and c_n non-urgent beds, for a total capacity of $c = c_u + c_n$ beds. Urgent patients occupy urgent beds first, with preemptive priority over non-urgent patients if this capacity is exceeded, while non-urgent patients are restricted to non-urgent beds. That is, urgent patients wait only for other urgent patients if all c beds are occupied by urgent patients, whereas non-urgent patients wait behind all urgent patients (both in service and queue) in addition to preceding non-urgent patients. Since the number of non-urgent patients is constrained by the balking threshold k , overall system stability is ensured solely by the stability of the urgent queue. Consequently, the ED system is stable when $\rho_u = \frac{\lambda_u}{c\mu_u} < 1$.

3.3. Optimization Problem. The objective is to determine the optimal alternative care threshold θ that maximizes the net benefit $Z(\theta)$, defined as:

$$Z(\theta) = aR(\theta) - bB(\theta) - cW(\theta), \quad (1)$$

where $R(\theta)$, $B(\theta)$, and $W(\theta)$ denote the long-run time averaged revenue, balking cost, and waiting cost, respectively under the alternative care threshold θ . The parameters a , b , and c weight the relative importance of these components and reflect managerial or institutional priorities. For clarity of exposition, we set $a = b = c = 1$ in the numerical analysis, but alternative weights can be used to represent different policy preferences. From the perspective of ED management, the objective is

to identify the optimal alternative care threshold θ^* that maximizes overall net benefit:

$$\theta^* = \arg \max_{\theta \in \{0, \dots, k-1\}} Z(\theta). \quad (2)$$

This optimization problem captures the trade-offs among revenue from ED and alternative care services, congestion-induced patient balking costs, and waiting costs associated with system delays. The finite feasible set for θ allows direct enumeration of candidate policies.

3.4. Stationary Analysis Framework. The two-class queuing system described above can be represented as a Quasi-Birth-Death (QBD) chain. All performance measures in this study are computed from the stationary distribution of the corresponding QBD chain. Since the objective function components are defined as long-run time averages, the ergodic theorem ensures that these quantities converge to steady-state expectations.

Formally, for any system metric $H(t)$ observed at time t , we have:

$$\lim_{T \rightarrow \infty} \frac{1}{T} \int_0^T H(t) dt = E[H] = \sum_{i=0}^{\infty} \sum_{j=0}^{k-1} H(i, j) \cdot \pi(i, j),$$

where $\pi(i, j)$ denotes the stationary probability of i urgent and j non-urgent patients in the system, and H is the steady-state random variable corresponding to $H(t)$. This stationary analysis framework allows us to evaluate all objective function components exactly as steady-state expectations under a given threshold policy θ , without the need to consider transient system behavior.

3.5. Objective Function Components. Using the stationary distribution $\pi(i, j)$, each component of the objective function $Z(\theta)$ can be expressed as a steady-state expectation.

3.5.1. Average Revenue. We decompose revenue into revenue generated by urgent patients, denoted by R_u , and those generated by non-urgent patients, denoted by $R_n(\theta)$ where the latter is affected by the particular threshold policy θ . $R_n(\theta)$ can be further decomposed as revenue generated from non-urgent patients treated in the ED and revenue from accepted alternative-care referrals. Define $D_u(t)$, $D_n(t)$ and $X^{\text{Alt}}(t)$ to be the cumulative number of urgent ED departures, non-urgent ED departures and accepted alternative-care referrals by time t . Then the long-run time-averaged revenue rate is:

$$R(\theta) = R_u + R_n(\theta), \quad (3)$$

where by the ergodic property of continuous time Markov chains

$$R_u = \lim_{T \rightarrow \infty} \frac{1}{T} [r_u^{\text{ED}} \cdot D_u(T)] = r_u^{\text{ED}} \cdot E[D_u],$$

and

$$\begin{aligned} R_n(\theta) &= R_n^{\text{ED}}(\theta) + R_n^{\text{Alt}}(\theta) = \lim_{T \rightarrow \infty} \frac{1}{T} [r_n^{\text{ED}} \cdot D_n(T) + r^{\text{Alt}} \cdot X^{\text{Alt}}(T)] \\ &= r_n^{\text{ED}} \cdot E[D_n] + r^{\text{Alt}} \cdot E[X^{\text{Alt}}]. \end{aligned} \quad (4)$$

Here $E[D_u]$, $E[D_n]$ and $E[X^{\text{Alt}}]$ are steady-state event rates. By PASTA

$$E[X^{\text{Alt}}] = \lambda_n \cdot p_a \cdot P(\theta \leq N < k),$$

where $P(\cdot)$ is the steady-state probability of the number N in the system. To express the steady-state non-urgent ED departure rate, let N_n^s denote the steady-state number of non-urgent patients in service. Then

$$E[D_n] = \mu_n \cdot E[N_n^s].$$

Here the steady-state expected number of non-urgents in service is:

$$E[N_n^s] = E[\min\{c - N_u^s, N_n, c_n\}],$$

where N_n is the number of non-urgents in system, and $N_u^s = \min\{c, N_u\}$ is the number of urgent patients in service. An analogous expression can be used for $E[D_u] = \mu_u \cdot E[N_u^s]$.

3.5.2. Average Balking Cost. Let $B_n(t)$ denote the cumulative number of balking non-urgent patients until time t . Then the long-run time-averaged balking cost rate is:

$$B(\theta) = \lim_{T \rightarrow \infty} \frac{1}{T} [c^b \cdot B_n(T)] = c^b \cdot E[B_n], \quad (5)$$

where c^b is the cost associated with each balking patient and $E[B_n]$ is the steady-state balking rate. By PASTA, $E[B_n] = \lambda_n \cdot P(N \geq k)$ and therefore

$$B(\theta) = c^b \cdot E[B_n] = c^b \cdot \lambda_n \cdot P(N \geq k),$$

and $P(N \geq k)$ is the steady-state probability that the system exceeds the balking threshold k .

3.5.3. Average Waiting Cost. For non-urgent patients, the average waiting cost is evaluated by the long-run time-averaged waiting cost rate:

$$W_n(\theta) = \lim_{T \rightarrow \infty} \frac{1}{T} \int_0^T [c_n^w \cdot N_n(t)] dt,$$

where $N_n(t)$ is the instantaneous number of non-urgent patients in the system at time t , including those in the queue and those receiving service, while c_n^w denotes the waiting cost rate per patient per unit time. This time-averaged formulation simplifies under the steady-state distribution to a function of the expected individual delay:

$$W_n(\theta) = c_n^w \cdot E[W_n], \quad (6)$$

In this expression, $E[W_n]$ is the expected time a non-urgent patient spends in the system under stationarity. This value is related to the expected number of non-urgent patients in the system, $E[N_n]$, via Little's law:

$$E[W_n] = E[N_n]/\lambda_n^{\text{eff}},$$

where λ_n^{eff} is the effective arrival rate of non-urgent patients who join the ED queue after accounting for those who balk or accept alternative care redirections. The long-run average waiting cost rate for urgent patients, W_u can be calculated in a similar way.

4. METHODOLOGY

4.1. Finding Steady-State Distribution. Our multi-class preemptive-priority queuing system can be represented as a level-dependent process where each level i corresponds to the number of urgent patients currently in the system. Within each level i , the phase j represents the number of

non-urgent patients in the system, where $j \in \{0, 1, \dots, k-1\}$. The system state is thus characterized by the pair (i, j) , where i represents the number of urgent patients currently in the system (defining the level), and j represents the number of non-urgent patients in the system (defining the phase within that level).

This structure allows us to model the system as a Quasi-Birth-Death (QBD) process following the approach developed by [Kao and Narayanan \(1991\)](#) for modeling multiprocessor systems with preemptive priorities. For the sake of completeness, we provide the QBD background modified to our case. The matrices A , B , and C were general in the original formulation in [Kao and Narayanan \(1991\)](#), but we have modified them to suit our specific multi-class emergency department queuing system. We will solve for the steady state distribution of our multi-class queuing system using a QBD process with the generator matrix Q :

$$Q = \begin{bmatrix} A_0 & B & & & & & & \\ C_1 & A_1 & B & & & & & \\ & C_2 & A_2 & B & & & & \\ & & \ddots & \ddots & \ddots & & & \\ & & & C_{h-1} & A_{h-1} & B & & \\ & & & & C & A & B & \\ & & & & C & A & B & \\ & & & & & \ddots & \ddots & \ddots \end{bmatrix}$$

where all blocked matrices are $k \times k$ and $h = \max(k, c)$.

4.1.1. Matrix Component Definitions. The block matrices in the QBD structure represent different types of transitions:

- (i) $B = \lambda_u I_k$ represents urgent arrivals that increase the level from i to $i + 1$. This matrix is level-independent since urgent arrivals occur at rate λ_u regardless of the current system state.
- (ii) $C_i = \mu_u \min\{i, c\} \cdot I_k$ (with $C = \mu_u \cdot c \cdot I_k$ for $i \geq c$) denotes urgent departures that decrease the level from i to $i - 1$. The service rate depends on the minimum of urgent patients present and available servers.
- (iii) the matrix A_i is tridiagonal for $i < h$ and captures transitions within level i , including non-urgent arrivals (when system capacity allows), non-urgent departures (when servers are available), and diagonal elements ensuring row sums equal zero, with:

$$\begin{aligned} a_{j,j+1}^{(i)} &= \lambda_n \alpha(i, j), \\ a_{j,j-1}^{(i)} &= \mu_n \min\{\max\{0, c - i\}, j, c_n\}, \\ a_{j,j}^{(i)} &= -(\lambda_u + \lambda_n \alpha(i, j) + \mu_u \min\{i, c\} + \mu_n \min\{\max\{0, c - i\}, j, c_n\}). \end{aligned}$$

Here

$$\alpha(i, j) = \begin{cases} 1 & \text{if } i + j < \theta, \\ 1 - p_a & \text{if } \theta \leq i + j < k, \\ 0 & \text{if } i + j \geq k. \end{cases}$$

For $i \geq h$, $A_i = A$ reflects only urgent dynamics.

We define the steady-state distribution as

$$\mathbf{X} = [\mathbf{x}_0, \mathbf{x}_1, \mathbf{x}_2, \dots]$$

where each \mathbf{x}_i represents the steady-state probability of being in level i :

$$\mathbf{x}_i = [x_{i,0}, x_{i,1}, \dots, x_{i,k-1}]_{1 \times k}$$

4.1.2. *Repeating Levels.* To find the steady-state distribution for $i \geq h$, we can express them as:

$$\mathbf{x}_i = \mathbf{x}_h \rho_u^{i-h}, \text{ where } \rho_u = \frac{\lambda_u}{c \cdot \mu_u}, \quad (7)$$

and where \mathbf{x}_h is the steady-state probability at level h .

4.1.3. *Boundary Levels.* For $i = 0, \dots, h-1$, we use a recursive approach.

For level 0:

$$\mathbf{x}_0 A_0 + \mathbf{x}_1 C_1 = \mathbf{0}$$

This equation represents the balance condition at level 0, where the first term captures within-level transitions (non-urgent arrivals and departures when no urgent patients are present), and the second term represents urgent departures from level 1 that bring the system back to level 0. For levels $i = 1, \dots, h-1$:

$$\mathbf{x}_{i-1} B_i + \mathbf{x}_i A_i + \mathbf{x}_{i+1} C_{i+1} = \mathbf{0}$$

where the first term represents arrivals from level $i-1$, the second term captures within-level transitions at level i , and the third term accounts for departures from level $i+1$.

$$\mathbf{x}_{i-1} B + \mathbf{x}_i A + \mathbf{x}_{i+1} C_{i+1} = \mathbf{0}$$

For level h :

$$\mathbf{x}_{h-1} B + \mathbf{x}_h A + \mathbf{x}_{h+1} C = \mathbf{0}$$

Substituting $\mathbf{x}_{h+1} = \mathbf{x}_h \rho_u$, we get:

$$\mathbf{x}_{h-1} B + \mathbf{x}_h (A + \rho_u C) = \mathbf{0}$$

Looking at the above equations, we can solve for each \mathbf{x}_i in terms of \mathbf{x}_{i+1} . The steady state distribution is obtained using the methodology as described by [Kao and Narayanan \(1991\)](#). The detailed recursive solution steps are provided in [Appendix A](#). The algorithm for determining steady-state and evaluating queue metrics is provided in [Appendix B](#).

4.2. **Validation of QBD Approach.** We validate the QBD Algorithm 1-2 for the Emergency Department model by comparing the marginal steady state probabilities, denoted $\pi(i)$ for the urgent

patients, obtained via QBD against the theoretical values from an $M/M/c$ queuing model only. The QBD marginal probabilities are computed by summing $\pi(i, j)$ for each state i (number of urgent patients) across all valid j (number of non-urgent patients) up to the balking threshold k . The comparison is performed for a range of states i , and the absolute and relative errors are calculated for each state. The validation results demonstrate extremely small relative and absolute errors, indicating high numerical accuracy of the QBD solver and confirming that the computed marginal probabilities closely match the theoretical $M/M/c$ probabilities.

4.3. Implementation of Objective Function Components. The objective function components from Section 4 are implemented using the steady-state distribution $\pi(i, j)$ obtained from the QBD model.

4.3.1. Average Revenue Implementation. The average revenue $R(\theta)$ from equation (3) is evaluated by computing $R_n^{\text{ED}}(\theta)$, and $R_n^{\text{Tele}}(\theta)$ separately using the formulae in (4). Note that

$$E[N_n^s] = \sum_{i=0}^{\infty} \sum_{j=0}^{k-1} s_n(i, j) \cdot \pi(i, j),$$

where $s_n(i, j) = \min\{j, \max\{0, c - i\}, c_n\}$, and

$$P(\theta \leq N < k) = \sum_{i=0}^{k-1} \sum_{j=\max(0, (\theta-i))}^{k-i-1} \pi(i, j)$$

4.3.2. Average Balking Cost Implementation. The average balking cost $B(\theta)$ is computed using (5) where-in the steady-state balking probability

$$P(N \geq k) = \sum_{i=0}^{\infty} \sum_{j=\max(0, k-i)}^{k-1} \pi(i, j) = \pi_f + \pi_g$$

where

$$\pi_f = \sum_{i=0}^{h-1} \sum_{j=\max(0, k-i)}^{k-1} \pi(i, j) \text{ and } \pi_g = \sum_{i=h}^{\infty} \sum_{j=\max(0, k-i)}^{k-1} \pi(i, j).$$

In order to compute π_g we use the geometric structure (7) for the tail of the steady state probabilities. Since $\pi(i, j) = x_{h,j} \cdot \rho_u^{i-h}$ for $i \geq h$ and $h = \max(k, c) \geq k$, we have:

$$\pi_g = \sum_{i=h}^{\infty} \sum_{j=0}^{k-1} x_{h,j} \cdot \rho_u^{i-h} = \sum_{j=0}^{k-1} x_{h,j} \sum_{i=h}^{\infty} \rho_u^{i-h} = \left(\sum_{j=0}^{k-1} x_{h,j} \right) \cdot \frac{1}{1 - \rho_u}$$

where the geometric series $\sum_{i=h}^{\infty} \rho_u^{i-h} = \frac{1}{1 - \rho_u}$ converges since $\rho_u < 1$ for system stability.

4.3.3. Average Waiting Cost Implementation. The average waiting cost $W(\theta)$ is calculated using equation (6), where $E[N_n] = \sum_{i=0}^{\infty} \sum_{j=0}^{k-1} j \cdot \pi(i, j)$.

The optimization algorithm evaluates the objective function from equation (1) across all feasible alternative care threshold values $\theta \in \{0, \dots, k-1\}$ to determine the optimal policy from equation (2).

4.4. Computational Results and Visualization: Rural and Urban. Emergency departments operate differently depending on their location and the populations they serve. Based on research

on rural-urban healthcare differences (Greenwood-Ericksen et al., 2019), we study two types of EDs: *rural* and *urban*. Each type faces unique challenges and has different resources available. Urban EDs serve more patients and have access to more resources. Rural EDs handle fewer patients but play a critical role in providing healthcare access to their communities. We base our input parameters on several references including national healthcare data (Cairns and Kang, 2024), emergency department performance studies (Canellas et al., 2023), and research on ED operations and costs (FairHealth Consumer, 2024).

TABLE 1. Emergency Department Input Parameters by Geographic Setting (Based on Literature)

Parameter	Unit	Rural ED	Urban ED	Ref.
Arrival rate (λ)	patients/hour	≈ 2	≈ 5	Cairns and Kang (2024); Association (2025)
Urgent proportion (p_u)	-	0.39	0.85	Alnasser et al. (2023); Patel et al. (2024)
Urgent service rate (μ_u)	patients/hour	0.15	0.15	Canellas et al. (2023); Cairns and Kang (2024)
Non-urgent service rate (μ_n)	patients/hour	0.32	0.32	Canellas et al. (2023); Cairns and Kang (2024)
Total beds (c)	beds	≈ 9	34	Greenwood-Ericksen et al. (2019)
Bed allocation ratio (c_u/c)	-	≈ 0.4	≈ 0.4	Mermiri et al. (2021)
Alternative care acceptance rate (p_a)	-	0.52	0.52	Weinick et al. (2010)
ED revenue - non-urgent (r_n^{ED})	\$/patient	675.50	675.50	FairHealth Consumer (2024)
ED revenue - urgent (r_u^{ED})	\$/patient	2,221.00	2,221.00	FairHealth Consumer (2024)
alternative care revenue (r^{Tele})	\$/patient	116.50	116.50	FairHealth Consumer (2024)
Alternative option revenue (r^{Alt})	\$/patient	436.00	436.00	FairHealth Consumer (2024)
Balking cost w.r.t. r^{Tele} (c^b)	\$/patient	384.82	384.82	Centers for Medicare & Medicaid Services (2024); Weinick et al. (2010); FairHealth Consumer (2024)
Balking cost w.r.t. r^{Alt} (c^b)	\$/patient	550.96	550.96	Centers for Medicare & Medicaid Services (2024); Weinick et al. (2010); FairHealth Consumer (2024)
Urgent waiting cost (c_u^w)	\$/hour	5,531.61	5,531.61	Cairns and Kang (2024); Liu et al. (2017); Grosse et al. (2019)
Non-urgent waiting cost (c_n^w)	\$/hour	53.21	53.21	Canellas et al. (2023); Rathlev et al. (2020)

The computational analysis is performed on these two representative ED configurations to demonstrate the model's applicability across different healthcare settings. Parameter values in Table 1 are derived from published healthcare data, with detailed derivations provided in Appendix C.

The implementation results and visualizations for these parameter sets are presented below as Rural ED Setting (Parameter Set 1) and Urban ED setting (Parameter Set 2). Since changing the alternative care threshold does not affect urgent patients, we plot the objective function components only for non-urgent patients with respect to threshold θ . Here we present the sensitivity analysis for Alternative Care.

4.4.1. *Rural ED Setting.* Using parameters from Table 1 (Rural ED column), the state space encompasses $j \in [0, 36]$ representing 37 non-urgent states, and the system remains stable with $\rho_u < 1$. Performance measures for this scenario at the optimal threshold $\theta^* = 5$ show $E[N_n] = 11.08$ as

the expected non-urgent patients in system, $\lambda_n^{eff} = 1.01$ as the effective non-urgent arrival rate, $E[W_n] = 10.97$ as the expected non-urgent waiting time, with an average of 3.15 non-urgent patients in service and a balking probability of $p_{balk} = 0.01$.

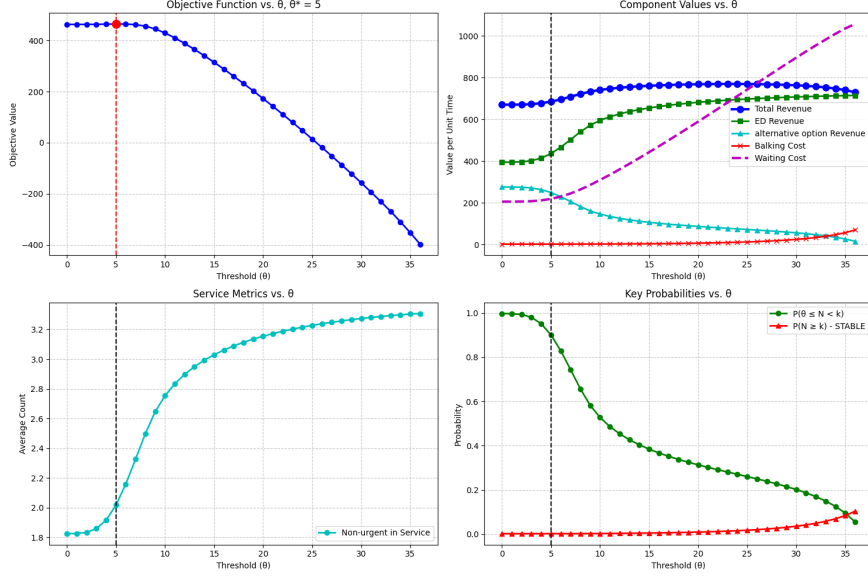


FIGURE 1. Rural ED Setting - Optimization Overview: Objective function vs. θ with optimal $\theta^* = 5$, showing component values, service metrics, and key probabilities

We report the expected relative error using exact $M/M/c$ probabilities as weights. The expected relative error is 1.825×10^{-7} .

4.4.2. Urban ED Setting. With parameters specified in Table 1 for the Urban ED setting, the state space encompasses $j \in [0, 38]$ representing 39 non-urgent states, and the system remains stable with

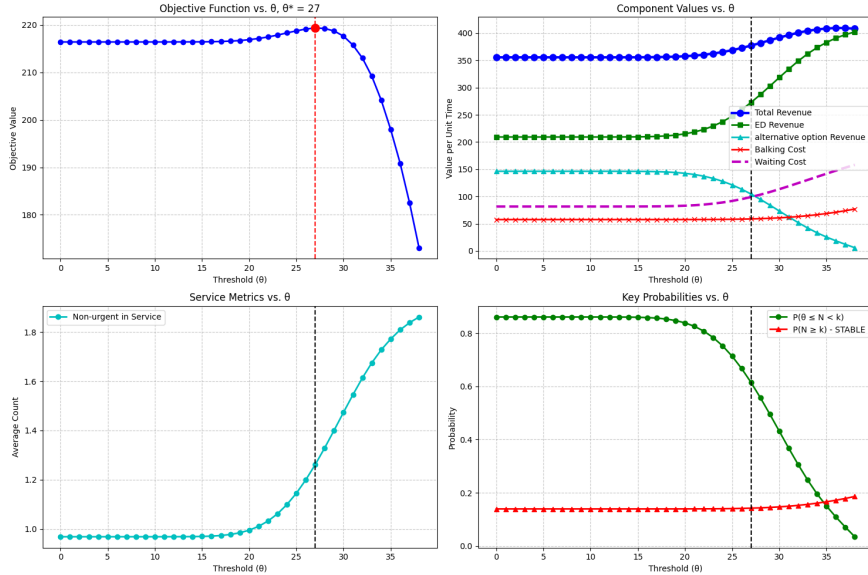


FIGURE 2. Urban ED setting - Optimization Overview: Objective function vs. θ with optimal $\theta^* = 27$, showing component values, service metrics, and key probabilities

$\rho_u < 1$. Performance measures for this scenario at the optimal threshold $\theta^* = 27$ show $E[N_n] = 1.56$ as the expected non-urgent patients in the system, $\lambda_n^{eff} = 0.32$ as the effective non-urgent arrival rate, $E[W_n] = 4.90$ as the expected non-urgent waiting time, with an average of 0.99 non-urgent patients in service and a balking probability of $p_{balk} = 0.14$. The expected relative error for the urban ED setting is 1.063×10^{-7} .

5. SENSITIVITY ANALYSIS

5.1. Tornado Diagram Analysis. To assess the robustness of the optimal alternative care threshold policy, we conduct a comprehensive sensitivity analysis using tornado diagrams. This analysis evaluates how parameter uncertainties affect the objective function $Z(\theta)$ at the optimal operating point $\theta^* = \arg \max_{\theta \in \{0, 1, \dots, k-1\}} Z(\theta)$ from equation (1). The sensitivity analysis considers the complete objective function including all performance metrics and components for both patient types: revenue from urgent and non-urgent patients (ED and telemedicine), waiting costs for urgent and non-urgent patients, and balking cost of non-urgents. This comprehensive approach captures the full system dynamics and trade-offs across all operational dimensions. Let \mathcal{P} denote the set of all parameters under consideration. For each parameter $p_i \in \mathcal{P}$, we compute:

$$\begin{aligned}\Delta_{\text{low}}^{(i)} &= Z(\theta^*; p_1^0, \dots, p_{i,\text{low}}, \dots, p_n^0) - Z_0 \\ \Delta_{\text{high}}^{(i)} &= Z(\theta^*; p_1^0, \dots, p_{i,\text{high}}, \dots, p_n^0) - Z_0 \\ I^{(i)} &= |\Delta_{\text{high}}^{(i)} - \Delta_{\text{low}}^{(i)}|\end{aligned}$$

where Z_0 is the baseline objective function value.

5.1.1. Methodology. Our tornado analysis evaluates sensitivity using operational ratios rather than individual parameters, comparing our alternative care threshold model against a no-referral baseline case. The analysis employs a comprehensive set of proportional relationships including bed allocation ratio (c_u/c), service rate ratio (μ_u/μ_n), revenue ratio (r_u^{ED}/r_n^{ED}), waiting cost ratio (c_u^w/c_n^w), alternative care revenue ratio (r^{Alt}/r_n^{ED}), balking cost ratio (c^b/r_n^{ED}), and threshold proportion (θ/k). For each operational ratio r_i , the sensitivity impact is computed as:

$$I^{(i)} = |Z(r_{i,\text{high}}) - Z(r_{i,\text{low}})|$$

where $r_{i,\text{low}} = r_i \cdot 0.95$ and $r_{i,\text{high}} = r_i \cdot 1.05$.

The analysis generates comprehensive tornado plots for two operational modes. First, for our alternative care-enabled ED model operating at optimal threshold θ^* , we provide tornado plots beginning with the base case (parameter set 1/2), then systematically varying each operational ratio by 20% in their feasible region to assess high and low sensitivity scenarios while fixing other ratios, incorporating both urgent and non-urgent revenue streams and associated costs. Second, for the alternative care-disabled case where all non-urgent patients enter the ED if $N(t) < k$ without alternative care options, we apply the same procedure. This comparative approach reveals differential sensitivity patterns between our alternative care policy and traditional ED operations, identifying which operational ratios exert the greatest influence on system performance and demonstrating the

robustness of our threshold policy across varying proportional configurations. We do our analyses separately for rural and urban ED settings.

5.2. Rural ED. This section presents the sensitivity analysis results examining how parameter variations affect the Rural ED model's performance.

5.2.1. Rural Alternative Care-enabled ED: Base Case. We use parameter values and key operational ratios from Table 1: $\lambda = 2$ patients/hour, $p_u = 0.39$, total capacity $c = 9$ beds, $k = 37$ patients, $p_a = 0.52$, bed allocation ratio ($c_u/c = 0.4$), service rate ratio ($\mu_u/\mu_n = 0.15/0.32$), revenue ratio ($r_u^{ED}/r_n^{ED} = 2,221/675.50$), waiting cost ratio ($c_u^w/c_n^w = 5,531.61/53.21$), alternative care revenue ratio ($r^{Alt}/r_n^{ED} = 436/675.50$), and balking cost ratio ($c^b/r_n^{ED} = 550.96/675.50$).

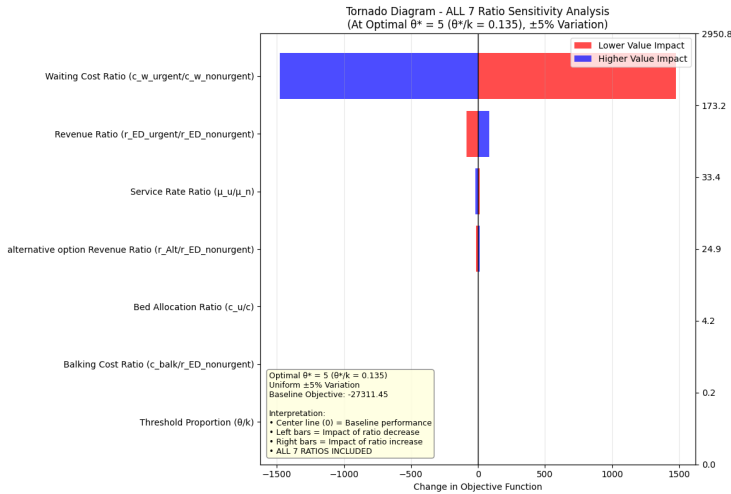


FIGURE 3. Tornado Diagram for Rural Alternative Care-enabled ED- ($\pm 5\%$ Variation)

TABLE 2. Sensitivity Analysis Summary - Rural Alternative Care-enabled ED

Rank	Ratio	Relative Impact (%)	Base Value
1	Waiting Cost Ratio (c_u^w/c_n^w)	10.81	103.958
2	Revenue Ratio (r_u^{ED}/r_n^{ED})	0.63	3.288
3	Service Rate Ratio (μ_u/μ_n)	0.12	0.469
4	Alternative Option Revenue Ratio (r^{Alt}/r_n^{ED})	0.09	0.645
5	Bed Allocation Ratio (c_u/c)	0.02	0.400
6	Balking Cost Ratio (c^b/r_n^{ED})	0.00	0.816
7	Threshold Proportion (θ/k)	0.00	0.135

5.2.2. Rural Alternative Care-enabled ED: Case Comparison. To understand how system characteristics affect sensitivity patterns, we analyze tornado diagrams across 15 different operational scenarios, ranging from high-demand to capacity-constrained systems.

TABLE 3. Case Comparison Summary for Rural Alternative Care-enabled ED

Rank	Case	Description	Baseline Obj	θ^*	θ^*/k	Top Ratio	Rel. Impact (%)
1	Low Urgent Proportion	$p_u - 20\%$	-21,154.99	6	0.162	c_u^w/c_n^w	10.95
2	Low Arrival Rate	$\lambda - 20\%$	-21,311.17	8	0.216	c_u^w/c_n^w	10.87
3	High Urgent Service Rate	$\mu_u + 20\%$	-21,837.87	8	0.216	c_u^w/c_n^w	11.07
4	High Capacity	$c + 20\%$	-26,759.90	8	0.216	c_u^w/c_n^w	10.85

Rank	Case	Description	Baseline Obj	θ^*	θ^*/k	Top Ratio	Rel. Impact (%)
5	Low Capacity	$c - 20\%$	-26,759.90	8	0.216	c_u^w/c_n^w	10.85
6	High Acceptance Rate	$p_a + 20\%$	-27,268.20	6	0.162	c_u^w/c_n^w	10.82
7	Low Balking Threshold	$k - 20\%$	-27,309.15	5	0.135	c_u^w/c_n^w	10.81
8	Baseline	Original parameters	-27,311.45	5	0.135	c_u^w/c_n^w	10.81
9	High Lambda	$\lambda + 20\%$	-27,311.45	5	0.135	c_u^w/c_n^w	10.81
10	High Theta	$\theta + 20\%$	-27,311.45	5	0.135	c_u^w/c_n^w	10.81
11	Low Theta	$\theta - 20\%$	-27,311.45	3	0.081	c_u^w/c_n^w	10.81
12	High Balking Threshold	$k + 20\%$	-27,317.46	3	0.081	c_u^w/c_n^w	10.80
13	Low Acceptance Rate	$p_a - 20\%$	-27,383.28	1	0.027	c_u^w/c_n^w	10.78
14	Low Urgent Service Rate	$\mu_u - 20\%$	-28,560.91	4	0.108	c_u^w/c_n^w	10.75
15	High Urgent Proportion	$p_u + 20\%$	-35,156.48	3	0.081	c_u^w/c_n^w	10.65

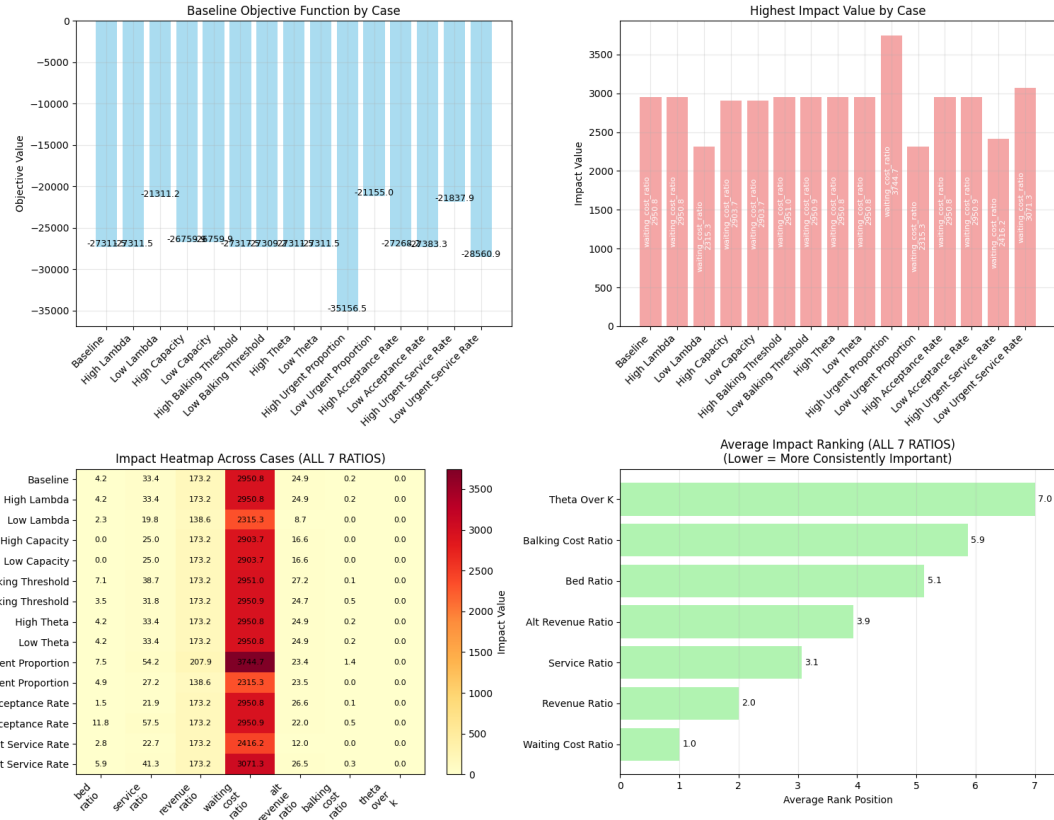


FIGURE 4. Case Comparison Summary of Rural Alternative Care-enabled ED: Baseline Objectives and Impact Rankings Across All Scenarios ($\pm 5\%$ Variation)

The sensitivity analysis across 15 scenarios reveals that the waiting cost ratio (urgent vs. non-urgent) dominates system performance, consistently accounting for 10-11% of the baseline objective function value across all cases. The patient mix emerges as the most critical operational factor: reducing urgent patients by 20% improves performance by 22.5%, while increasing them by 20% deteriorates performance by 28.7%. The optimal threshold θ^* varies substantially across scenarios, demonstrating the need for context-dependent policies. Revenue ratio provides consistent secondary impact, while service rate considerations remain tertiary. These findings highlight that managing patient mix and understanding relative waiting costs are the primary drivers of ED optimization.

5.2.3. *Rural Alternative Care-disabled ED: Base Case.* Here we consider a simplified emergency department model, that eliminates alternative care referrals entirely, creating a binary decision system where non-urgent patients either enter the ED (when total patients $< k$) or balk (when total patients $\geq k$). This streamlined approach again focuses exclusively on five core operational ratios: bed allocation ratio, service rate ratio, revenue ratio, waiting cost ratio, and balking cost ratio.

The base case configuration maintains the same fundamental parameters from Table 1: $\lambda = 2$ patients/hour, $p_u = 0.39$, total capacity $c = 9$ beds, $k = 37$ patients, with identical operational ratios as the alternative option-enabled model. However, the simplified balking function eliminates the intermediate alternative option. The probability that a non-urgent patient decides to join the ED upon arrival when the system state is (i, j) , denoted $\alpha(i, j)$, equals 1 when the total number of patients $(i + j)$ is below the threshold k , meaning non-urgent patients join the system. When the total reaches or exceeds k patients, $\alpha(i, j)$ equals 0, causing all non-urgent patients to balk and leave without receiving care.

This simplified baseline model serves as a useful comparison point to demonstrate the operational benefits that the alternative option provides in emergency department management.

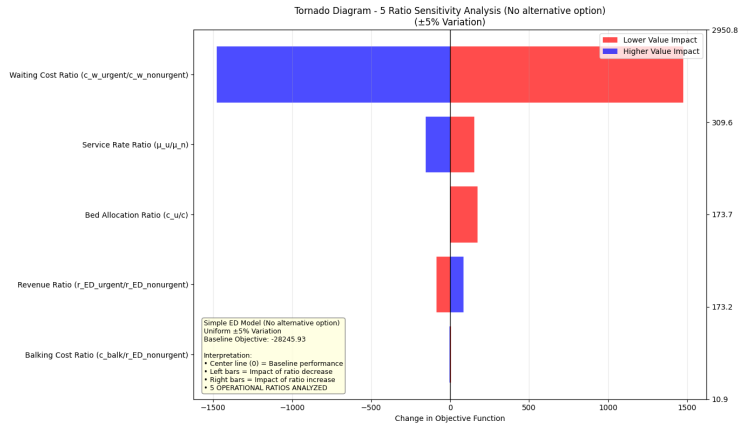


FIGURE 5. Tornado Diagram for Rural Alternative Care-disabled ED- ($\pm 5\%$ Variation)

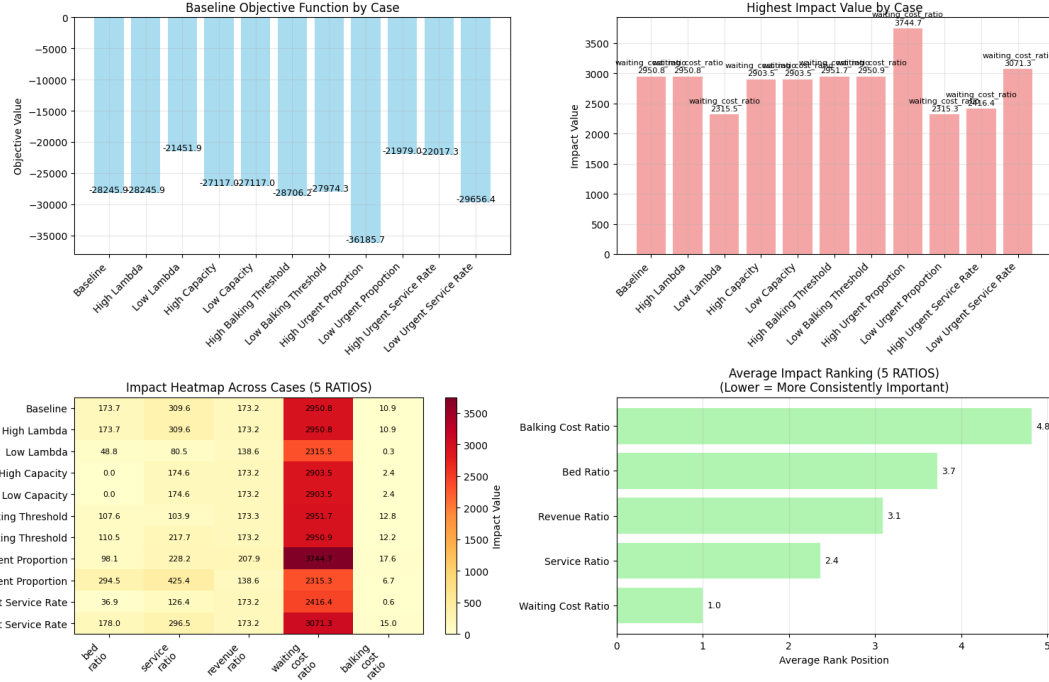
Rank	Ratio	Relative Impact (%)	Base Value
1	Waiting Cost Ratio (c_w^u/c_w^n)	10.45	103.958
2	Service Rate Ratio (μ_u/μ_n)	1.10	0.469
3	Bed Allocation Ratio (c_u/c)	0.62	0.400
4	Revenue Ratio (r_u^{ED}/r_n^{ED})	0.61	3.288
5	Balking Cost Ratio (c_b^{ED}/r_n^{ED})	0.04	1.000

TABLE 4. Sensitivity Analysis Summary - Rural Alternative Care-disabled ED

5.2.4. *Rural Alternative Care-disabled ED: Case Comparison.* To understand sensitivity patterns in the simplified model, we analyze tornado diagrams across 11 different operational scenarios, examining how system characteristics affect parameter importance without alternative care complexity.

TABLE 5. Case Comparison Summary for Rural Alternative Care-disabled ED

Rank	Case	Description	Baseline Obj	Top Ratio	Rel. Impact (%)
1	Low Arrival Rate	$\lambda - 20\%$	-21,451.87	c_u^w / c_n^w	10.79
2	Low Urgent Proportion	$p_u - 20\%$	-21,978.96	c_u^w / c_n^w	10.53
3	High Urgent Service Rate	$\mu_u + 20\%$	-22,017.27	c_u^w / c_n^w	10.97
4	High Capacity	$c - 20\%$	-27,117.04	c_u^w / c_n^w	10.71
5	Low Capacity	$c - 20\%$	-27,117.04	c_u^w / c_n^w	10.71
6	Low Balking Threshold	$k - 20\%$	-27,974.34	c_u^w / c_n^w	10.55
7	Baseline	Original parameters	-28,245.93	c_u^w / c_n^w	10.45
8	High Arrival Rate	$\lambda + 20\%$	-28,245.93	c_u^w / c_n^w	10.45
9	High Balking Threshold	$k + 20\%$	-28,706.18	c_u^w / c_n^w	10.28
10	Low Urgent Service Rate	$\mu_u - 20\%$	-29,656.36	c_u^w / c_n^w	10.36
11	High Urgent Proportion	$p_u + 20\%$	-36,185.67	c_u^w / c_n^w	10.35

FIGURE 6. Case Comparison Summary of Rural Alternative Care-disabled ED: Baseline Objectives and Impact Rankings Across All Scenarios ($\pm 5\%$ Variation)

In the absence of alternative care options, the waiting cost ratio remains the dominant factor, consistently accounting for 10-11% of baseline performance across all 11 scenarios. Service rate ratio emerges as the secondary factor, followed by revenue ratio as tertiary (average rank 3.1). Patient mix drives dramatic performance variation, with the worst-case scenario (high urgent proportion) performing 68.7% worse than the best-case (low arrival rate). Without alternative care pathways, service efficiency becomes more critical for managing system bottlenecks, though waiting cost differentials remain the primary optimization driver.

5.2.5. Rural ED: Alternative Care Enabled vs. Disabled. Alternative care improves performance across all 11 scenarios, with gains ranging from 0.66% (low arrival rate) to 4.84% (high balking threshold). Under baseline conditions, alternative care provides a 3.31% improvement, while maintaining consistent benefits even under high demand conditions (2.85% improvement in high urgent

proportion scenario). The waiting cost ratio remains the dominant factor (10-11% relative impact) in both configurations, indicating that alternative care enhances operational efficiency without altering the fundamental performance drivers.

TABLE 6. Alternative Care Impact: Enabled vs. Disabled with Relative Impact Comparison

Scenario	Enabled (\$/hr)	Enabled Rel. Impact (%)	Disabled (\$/hr)	Disabled Rel. Impact (%)	Benefit (\$/hr)	Gain (%)
Low Urgent Proportion	-21,155	10.95	-21,979	10.53	+824	+3.75
Low Arrival Rate	-21,311	10.87	-21,452	10.79	+141	+0.66
High Urgent Service Rate	-21,838	11.07	-22,017	10.97	+179	+0.81
High Capacity	-26,760	10.85	-27,117	10.71	+357	+1.32
Low Capacity	-26,760	10.85	-27,117	10.71	+357	+1.32
Low Balking Threshold	-27,309	10.81	-27,974	10.55	+665	+2.38
Baseline	-27,311	10.81	-28,246	10.45	+935	+3.31
High Arrival Rate	-27,311	10.81	-28,246	10.45	+935	+3.31
High Balking Threshold	-27,317	10.80	-28,706	10.28	+1,389	+4.84
Low Urgent Service Rate	-28,561	10.75	-29,656	10.36	+1,095	+3.69
High Urgent Proportion	-35,156	10.65	-36,186	10.35	+1,030	+2.85

5.3. **Urban ED.** The following section reports sensitivity analysis findings for the Urban ED model.

5.3.1. *Urban Alternative Care-enabled ED: Base Case.* We use parameter values and key operational ratios from Table 1 (Urban ED column) with the following key operational ratios: bed allocation ratio ($c_u/c = 0.4$), service rate ratio ($\mu_u/\mu_n = 0.15/0.32$), revenue ratio ($r_u^{ED}/r_n^{ED} = 2,221/675.50$), waiting cost ratio ($c_u^w/c_n^w = 5,531.61/53.21$), alternative care revenue ratio ($r^{Alt}/r_n^{ED} = 436/675.50$), and balking cost ratio ($c_b^b/r_n^{ED} = 550.96/675.50$).

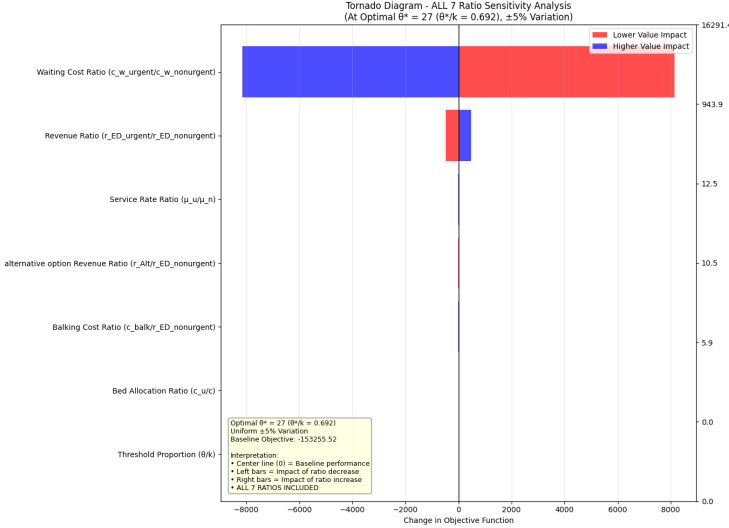
FIGURE 7. Tornado Diagram for Urban Alternative Care-enabled ED- ($\pm 5\%$ Variation)

TABLE 7. Sensitivity Analysis Summary - Urban Alternative Care-enabled ED

Rank	Ratio	Relative Impact (%)	Base Value
1	Waiting Cost Ratio (c_u^w/c_n^w)	10.63	103.958
2	Revenue Ratio (r_u^{ED}/r_n^{ED})	0.62	3.288
3	Service Rate Ratio (μ_u/μ_n)	0.01	0.469

Rank	Ratio	Relative Impact (%)	Base Value
4	Alternative Option Revenue Ratio (r^{Alt}/r_n^{ED})	0.01	0.645
5	Balking Cost Ratio (c^b/r_n^{ED})	0.004	0.816
6	Bed Allocation Ratio (c_u/c)	0.00	0.400
7	Threshold Proportion (θ/k)	0.00	0.692

5.3.2. *Urban Alternative Care-enabled ED: Case Comparison*. To understand how system characteristics affect sensitivity patterns, we analyze tornado diagrams across 15 different operational scenarios, ranging from high-demand to capacity-constrained systems.

Rank	Case	Description	Baseline Obj	Top Ratio	Rel. Impact (%)
1	Low Urgent Proportion	$p_u - 20\%$	295,179.19	μ_u/μ_n	107.89
2	High Arrival Rate	$\lambda + 20\%$	-58,761.64	c^w/c_n^w	10.67
3	Low Arrival Rate	$\lambda - 20\%$	-118,019.40	c_u^w/c_n^w	10.64
4	High Urgent Service Rate	$\mu_u + 20\%$	-121,156.43	c_u^w/c_n^w	10.81
5	High Urgent Proportion	$p_u + 20\%$	-127,689.06	c_u^w/c_n^w	10.77
6	High Capacity	$c + 20\%$	-147,308.09	c_u^w/c_n^w	10.66
7	High Balking Threshold	$k + 20\%$	-152,674.22	c_u^w/c_n^w	10.64
8	High Acceptance Rate	$p_a + 20\%$	-153,244.53	c_u^w/c_n^w	10.63
9	Baseline	Original parameters	-153,255.52	c_u^w/c_n^w	10.63
10	High Theta	$\theta + 20\%$	-153,255.52	c_u^w/c_n^w	10.63
11	Low Theta	$\theta - 20\%$	-153,255.52	c_u^w/c_n^w	10.63
12	Low Acceptance Rate	$p_a - 20\%$	-153,266.31	c_u^w/c_n^w	10.63
13	Low Balking Threshold	$k - 20\%$	-153,455.28	c_u^w/c_n^w	10.62
14	Low Urgent Service Rate	$\mu_u - 20\%$	-163,139.02	c_u^w/c_n^w	10.59
15	Low Capacity	$c - 20\%$	-349,628.58	c_u^w/c_n^w	10.26

TABLE 8. Case Comparison Summary for Urban Alternative Care-enabled ED

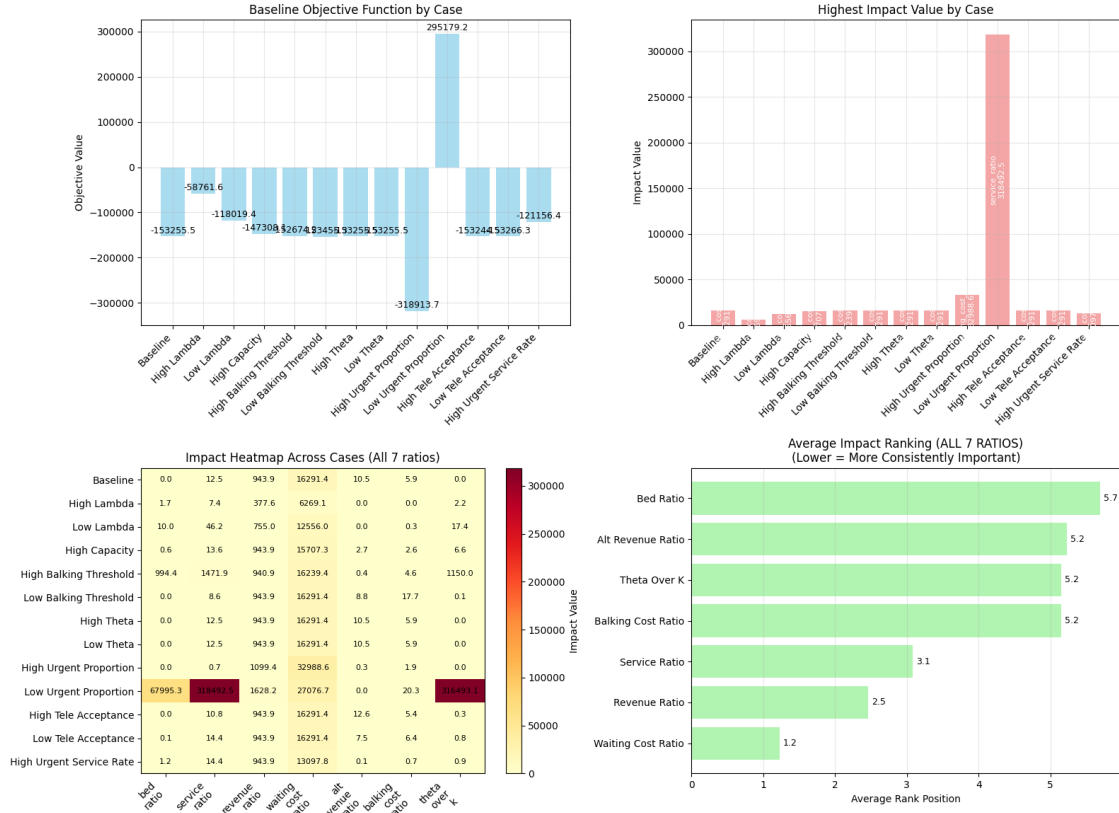


FIGURE 8. Case Comparison Summary of Urban Alternative Care-enabled ED: Baseline Objectives and Impact Rankings Across All Scenarios ($\pm 5\%$ Variation)

The waiting cost ratio dominates 14 of 15 scenarios, consistently accounting for 10-11% of baseline performance. However, the service rate ratio demonstrates exceptional sensitivity in the low urgent proportion scenario, far exceeding all other parameters, revealing that service efficiency becomes critical when urgent patient volumes are low and the system becomes revenue-positive. Revenue ratio provides consistent secondary impact (average rank 2.6), while threshold proportion and alternative revenue ratios show moderate importance. Performance varies dramatically across scenarios, with the worst case (low capacity) performing 218% worse than the best case (low urgent proportion), underscoring the critical importance of capacity management in urban EDs.

5.3.3. Urban Alternative Care-disabled ED: Base Case. Here we consider a simplified emergency department model, that eliminates alternative option referrals entirely, creating a binary decision system where non-urgent patients either enter the ED (when total patients $< k$) or balk (when total patients $\geq k$). This streamlined approach focuses exclusively on five core operational ratios: bed allocation ratio, service rate ratio, revenue ratio, waiting cost ratio, and balking cost ratio.

The base case configuration maintains the same fundamental parameters from Table 1 (Urban ED column) with identical operational ratios as the alternative option enabled model. However, the simplified balking function eliminates the intermediate alternative option. The probability that a non-urgent patient decides to join the ED upon arrival when the system state is (i, j) , denoted $\alpha(i, j)$, equals 1 when the total number of patients $(i + j)$ is below the threshold k , meaning non-urgent patients join the system. When the total reaches or exceeds k patients, $\alpha(i, j)$ equals 0, causing all non-urgent patients to balk and leave without receiving care.

This simplified baseline model serves as a useful comparison point to demonstrate the operational benefits that alternative option provides in emergency department management.

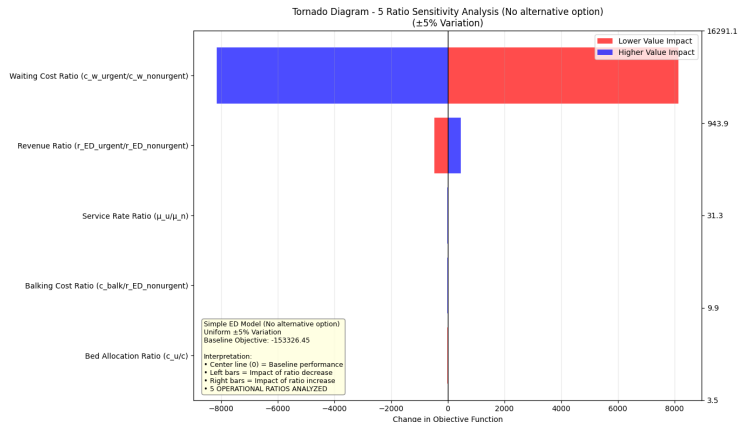


FIGURE 9. Tornado Diagram for Urban Alternative Care-disabled ED- ($\pm 5\%$ Variation)

Rank	Ratio	Relative Impact (%)	Base Value
1	Waiting Cost Ratio (c_u^w/c_n^w)	10.62	103.958
2	Revenue Ratio (r_u^{ED}/r_n^{ED})	0.62	3.288
3	Service Rate Ratio (μ_u/μ_n)	0.02	0.469
4	Balking Cost Ratio (c_b^{ED}/r_n^{ED})	0.006	1.000
5	Bed Allocation Ratio (c_u/c)	0.002	0.400

TABLE 9. Sensitivity Analysis Summary - Urban Alternative Care-disabled ED

5.3.4. *Urban Alternative Care-disabled ED: Case Comparison*. To understand sensitivity patterns in the simplified model, we analyze tornado diagrams across 11 different operational scenarios, examining how system characteristics affect parameter importance without alternative option complexity.

Rank	Case	Description	Baseline Obj	Top Ratio	Rel. Impact (%)
1	Low Urgent Proportion	$p_u - 20\%$	295,133.20	μ_u / μ_n	107.81
2	High Arrival Rate	$\lambda + 20\%$	-58,761.64	c_u^w / c_n^w	10.67
3	Low Arrival Rate	$\lambda - 20\%$	-118,020.27	c_u^w / c_n^w	10.64
4	High Urgent Service Rate	$\mu_u + 20\%$	-121,160.00	c_u^w / c_n^w	10.81
5	High Urgent Proportion	$p_u + 20\%$	-135,695.39	c_u^w / c_n^w	10.63
6	High Capacity	$c + 20\%$	-147,327.84	c_u^w / c_n^w	10.66
7	Baseline	Original parameters	-153,326.45	c_u^w / c_n^w	10.62
8	Low Balking Threshold	$k - 20\%$	-153,528.20	c_u^w / c_n^w	10.61
9	High Balking Threshold	$k + 20\%$	-154,898.62	c_u^w / c_n^w	10.62
10	Low Urgent Service Rate	$\mu_u - 20\%$	-163,239.64	c_u^w / c_n^w	10.58
11	Low Capacity	$c - 20\%$	-349,884.14	c_u^w / c_n^w	10.25

TABLE 10. Case Comparison Summary for Urban Alternative Care-disabled ED

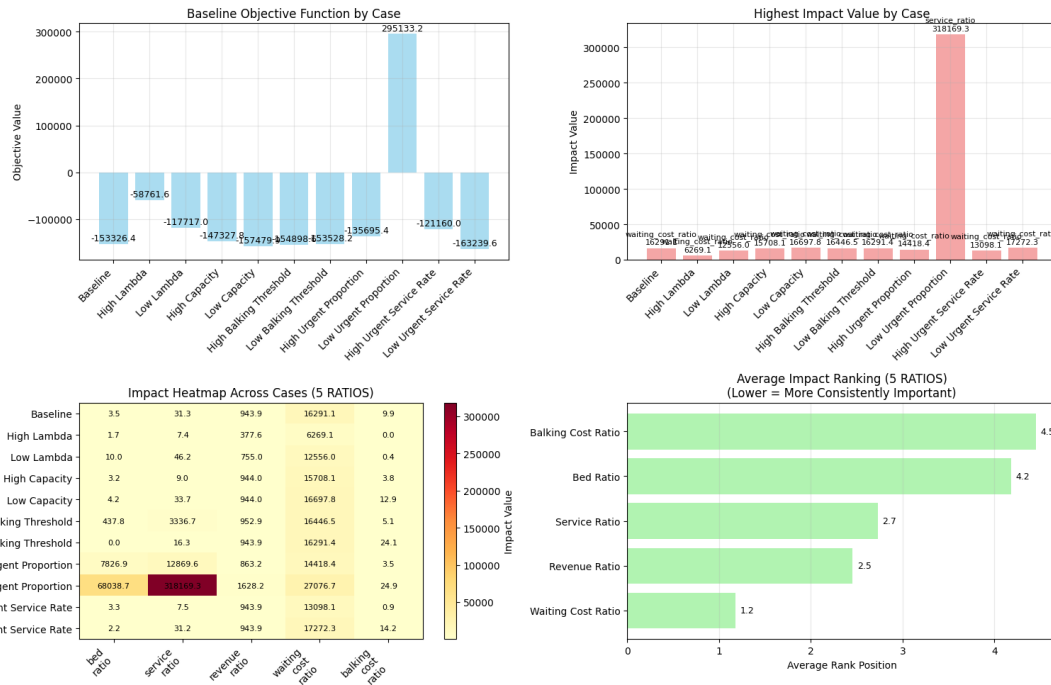


FIGURE 10. Case Comparison Summary of Urban Alternative Care-disabled ED: Baseline Objectives and Impact Rankings Across All Scenarios ($\pm 5\%$ Variation)

The waiting cost ratio dominates 10 of 11 scenarios, consistently accounting for 10-11% of baseline performance. The service rate ratio demonstrates exceptional sensitivity in the low urgent proportion scenario, the best-performing case where the system achieves positive revenue, far exceeding all other parameters. Revenue ratio provides consistent secondary impact (average rank 2.5), while bed allocation and balking cost ratios show minimal influence. Performance varies dramatically: the system performs 218% worse in the worst case (low capacity) compared to the best case (low urgent proportion), underscoring that patient mix and capacity management remain critical drivers even without alternative care pathways.

5.3.5. *Urban ED: Alternative Care Enabled vs. Disabled.* Alternative care improves or maintains performance across all 11 scenarios. Under baseline conditions, alternative care provides a 0.046% improvement. The largest benefit occurs under high urgent proportion conditions (5.90%), while high balking threshold scenarios show 1.44% improvement. The waiting cost ratio remains dominant (10-11% relative impact) in both configurations, while service rate ratio demonstrates exceptional importance in low urgent proportion scenarios, regardless of alternative care availability, indicating fundamental operational leverage points persist across configurations.

Scenario	Enabled (\$/hr)	Enabled Rel. Impact (%)	Disabled (\$/hr)	Disabled Rel. Impact (%)	Benefit (\$/hr)	Gain (%)
Low Urgent Proportion	+295,179	107.89	+295,133	107.81	+46	+0.016
High Arrival Rate*	-58,762	10.67	-58,762	10.67	+0	+0.000
Low Arrival Rate	-118,019	10.64	-118,020	10.64	+1	+0.001
High Urgent Service Rate	-121,156	10.81	-121,160	10.81	+4	+0.003
High Capacity	-147,308	10.66	-147,328	10.66	+20	+0.013
Low Balking Threshold	-153,455	10.62	-153,528	10.61	+73	+0.048
Baseline	-153,256	10.63	-153,326	10.62	+71	+0.046
High Balking Threshold	-152,674	10.64	-154,899	10.62	+2,224	+1.44
Low Urgent Service Rate	-163,139	10.59	-163,240	10.58	+101	+0.062
Low Capacity	-349,629	10.26	-349,884	10.25	+256	+0.073
High Urgent Proportion	-127,689	10.77	-135,695	10.63	+8,006	+5.90

*Arrival rate capped at $\lambda = 5$ (baseline value) due to system stability constraints

TABLE 11. Alternative Care Impact: Enabled vs. Disabled with Relative Impact Comparison

5.4. **Proportional Analysis: Optimal Objective Function Response.** To complement the tornado diagram sensitivity analysis, we conduct a comprehensive proportional analysis that examines how systematic variations in each operational ratio affect the optimal objective function. Unlike the tornado analysis which evaluates parameter sensitivity at a fixed threshold policy, the proportional analysis optimizes the alternative care threshold θ^* for each ratio configuration, revealing the true performance envelope under varying operational conditions.

5.4.1. *Methodology:* For each operational ratio in our comprehensive set $\mathcal{R} = \{\text{bed ratio, service ratio, revenue ratio, waiting cost ratio, alternative care revenue ratio, balking cost ratio, and } \theta/k\}$, we systematically vary each ratio across its feasible operating range while allowing the alternative care threshold policy to optimize freely for each configuration.

The analysis begins by establishing the practical bounds for each ratio based on operational constraints, then systematically exploring how changes in these fundamental operational relationships affect system performance when the threshold policy is allowed to adapt optimally. For each ratio configuration tested, we determine the threshold value that maximizes the objective function, record both the optimal threshold and the resulting performance level, and analyze the patterns that emerge across the ratio's feasible range.

This approach reveals how each operational ratio affects not just sensitivity (as shown in tornado analysis) but the actual optimal performance envelope when the system is allowed to adapt its alternative care policy dynamically.

5.4.2. *Rural Alternative Care-enabled ED: Base Case.* Under standard parameters (optimal $\theta^* = 5$), the system demonstrates balanced optimization with clear sensitivity patterns. Figure 14 shows the two most critical ratios; additional proportional sensitivity analyses are provided in Appendix D.

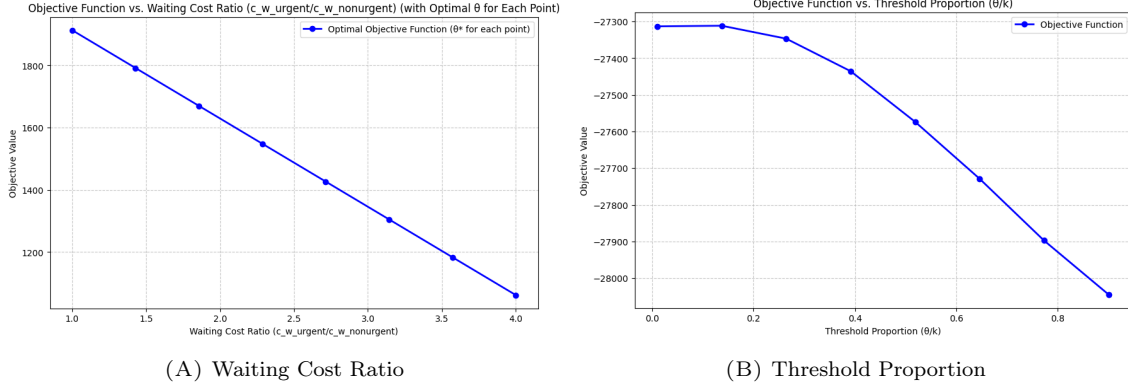


FIGURE 11. Baseline Case Analysis: Critical Sensitivity Ratios

The waiting cost ratio exhibits the most dramatic performance impact, with the objective function declining steeply and nearly linearly as the ratio increases. This indicates that as urgent patients incur proportionally higher waiting costs relative to non-urgent patients, the system performance deteriorates significantly, creating extreme cost penalties during delays. The threshold proportion shows performance remains relatively stable at low values of θ/k , then declines with increasing steepness at higher proportions. Higher thresholds force patients to wait longer before alternative care referral, accumulating higher waiting costs and increased balking, with performance dropping from approximately $-27,300$ to $-28,050$ as the proportion increases from 0 to 0.9.

5.4.3. Urban Alternative Care-enabled ED: Base Case. Under standard parameters (optimal $\theta^* = 27$), the system demonstrates balanced optimization with clear sensitivity patterns. Figure 14 shows the two most critical ratios; additional proportional sensitivity analyses are provided in Appendix D.

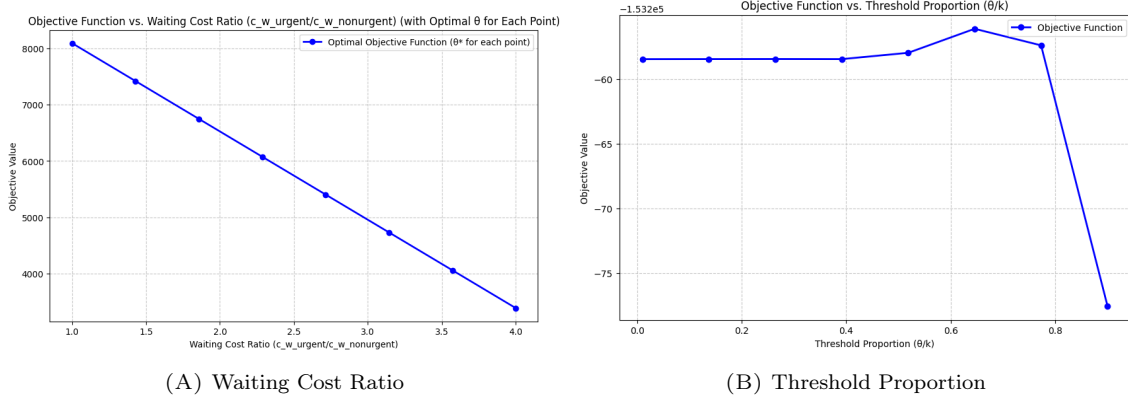


FIGURE 12. Baseline Case Analysis: Critical Sensitivity Ratios

The waiting cost ratio exhibits extreme performance impact, declining from approximately 8,091 at ratio 1.0 to 3,390 at ratio 4.0. As urgent patients incur proportionally higher waiting costs relative to non-urgent patients, the system performance deteriorates significantly, creating severe cost penalties during delays. The threshold proportion reveals a non-monotonic pattern distinct from rural EDs: performance remains stable for $\theta/k < 0.5$, slightly improves to peak at $\theta/k \approx 0.7$, then

collapses dramatically beyond $\theta/k \approx 0.75$. This pattern suggests that moderate-to-high thresholds can be optimal in urban settings before excessive waiting causes severe cost accumulation and balking.

6. CAPACITY ALLOCATION OPTIMIZATION

6.1. Capacity Allocation Problem. While the previous sections focused on optimizing the alternative care threshold θ for a fixed capacity allocation (c_u, c_n) , this section addresses the complementary problem of optimizing the capacity allocation itself. Given a total ED capacity $c = c_u + c_n$ and the previously determined optimal alternative care threshold θ^* , we seek to determine the optimal allocation of urgent beds c_u^* and non-urgent beds c_n^* that maximizes the system's net benefit $Z(c_u, c_n, \theta^*)$. Specifically, we define the optimal capacity allocation (c_u^*, c_n^*) as the solution to the optimization problem that determines how to optimally distribute the total available bed capacity between urgent and non-urgent patient care to achieve maximum system performance under the optimal alternative care referral policy.

The capacity allocation optimization problem can be formulated as:

$$(c_u^*, c_n^*) = \arg \max_{c_u, c_n} Z(c_u, c_n, \theta^*)$$

subject to:

$$c_u + c_n = c \quad (\text{total capacity constraint})$$

$$c_u, c_n \geq 0 \quad (\text{non-negativity constraints})$$

$$c_u, c_n \in \mathbb{Z}^+ \quad (\text{integer constraints})$$

where θ^* represents the optimal alternative care threshold for each given capacity allocation (c_u, c_n) .

6.1.1. Direct Capacity Optimization. Given the preemptive priority structure in our system, we employ direct optimization through complete enumeration. The algorithm is provided in Appendix B.

6.2. Nested vs. Fixed-partitioned Bed Configuration. To further evaluate the impact of capacity allocation strategies, we compared two bed configuration approaches. The comparison examines nested bed allocation (where urgent patients can overflow to non-urgent beds with preemptive priority) versus fixed bed allocation (where urgent and non-urgent patients are strictly assigned to their designated bed types).

The Fixed approach models the emergency department as two independent queues that interact only through the alternative care decision mechanism based on total system occupancy $(i + j)$.

(i) The urgent queue operates as a standard $M/M/c_u/\infty$ system with arrival rate $\lambda_u = \lambda \cdot p_u$, service rate μ_u , and traffic intensity $\rho_u = \lambda_u/\mu_u$, requiring stability condition $\rho_u/c_u < 1$. The steady-state probabilities follow $\pi_u(0) = [\sum_{n=0}^{c_u-1} \rho_u^n/n! + \rho_u^{c_u}/(c_u!(c_u - \rho_u))]^{-1}$, with $\pi_u(i) = \pi_u(0) \cdot \rho_u^i/i!$ for $0 \leq i \leq c_u$ and $\pi_u(i) = \pi_u(0) \cdot \rho_u^i/(c_u! \cdot c_u^{i-c_u})$ for $i > c_u$ (Shortle et al., 2018).

(ii) The non-urgent queue follows a birth-death process with state-dependent arrival rates $\lambda_j = \lambda_n \sum_{i=0}^{\infty} \pi_u(i) \cdot \alpha(i, j)$ where $\alpha(i, j)$ is defined in (iii) and death rates $\mu_j = \mu_n \cdot \min(j, c_n)$.

The steady-state probabilities are $\pi_n(j) = \pi_n(0) \prod_{m=0}^{j-1} \lambda_m / \mu_{m+1}$ with normalization $\pi_n(0) = [1 + \sum_{j=1}^{k-1} \prod_{m=0}^{j-1} \lambda_m / \mu_{m+1}]^{-1}$ (Crawford et al., 2018).

The solution algorithm begins by verifying urgent queue stability and solving the $M/M/c_u/\infty$ system to obtain $\{\pi_u(i)\}$, then calculates birth rates λ_j and death rates μ_j for the non-urgent birth-death process.

6.2.1. Computational Results. For stability analysis in rural and urban ED settings where $\rho_u < 1$, our results reveal significant differences in the number of feasible bed allocation configurations. In the rural setting with 9 total beds, only 3 out of 8 possible allocations achieve system stability (37.5% feasible). The system requires a minimum of 6 beds allocated to urgent patients to maintain stability. In contrast, the urban setting with 34 total beds exhibits much tighter stability constraints, with only 5 out of 33 possible allocations achieving stability (15.2% feasible). The urban system requires at least 29 beds allocated to urgent patients for stability. Due to the limited number of stable configurations in both settings, we introduce an alternative parameter set that yields a broader range of stable allocations, enabling a more comprehensive comparison between fixed and nested threshold policies.

We use this parameter set to compare fixed-partitioned versus nested approaches, as the rural and urban models exhibit instability under various bed configurations, limiting valid comparisons.

$\lambda = 20$, $p_u = 0.8$, $\mu_u = 4$, $\mu_n = 6$, $c_u = 8$, $c_n = 10$, $k = 25$, $\theta = 20$, $p_a = 0.5$, $r_n^{ED} = 100$, $r^{Tele} = 40$, $c^b = 30$, $c_n^w = 20$, $r_u^{ED} = 200$, $c_u^w = 30$.

TABLE 12. Detailed Comparison: NESTED vs FIXED-PARTITIONED Bed Configuration ($c_u = 8$, $c_n = 10$)

Bed Configuration: $c_u = 8$ urgent beds, $c_n = 10$ non-urgent beds				
Detailed Comparison Table (NESTED vs FIXED-PARTITIONED)				
θ	NESTED	FIXED	Diff	Better
0	3353.33	3278.24	75.09	NESTED
1	3354.69	3278.60	76.09	NESTED
2	3360.53	3280.16	80.37	NESTED
3	3373.22	3283.63	89.59	NESTED
4	3391.87	3288.91	102.96	NESTED
5	3412.73	3295.12	117.61	NESTED
6	3431.68	3301.11	130.57	NESTED
7	3446.21	3305.96	140.25	NESTED
8	3455.84	3309.31	146.53	NESTED
9	3461.45	3311.32	150.13	NESTED
10	3464.37	3312.41	151.96	NESTED
11	3465.74	3312.97	152.76	NESTED
12	3466.32	3313.26	153.06	NESTED
13	3466.55	3313.40	153.14	NESTED
14	3466.63	3313.48	153.15	NESTED
15	3466.65	3313.51	153.14	NESTED
16	3466.66	3313.53	153.13	NESTED
17	3466.67	3313.54	153.13	NESTED
18	3466.67	3313.54	153.12	NESTED
19	3466.67	3313.55	153.12	NESTED
20	3466.67	3313.55	153.12	NESTED
21	3466.67	3313.55	153.12	NESTED
22	3466.67	3313.55	153.12	NESTED
23	3466.67	3313.55	153.12	NESTED
24	3466.67	3313.55	153.12	NESTED

Summary: NESTED wins 25/25, FIXED-PARTITIONED wins 0/25, Ties 0/25

TABLE 13. Bed Combination Analysis: NESTED vs FIXED-PARTITIONED (Total Capacity: 18 beds)

Bed Combination Analysis (Total beds: 18)								
c_u	c_n	Total	NESTED θ^*	NESTED Obj	FIXED θ^*	FIXED Obj	Difference	Better
1	17	18	—	—	—	—	—	FIXED UNSTABLE
2	16	18	—	—	—	—	—	FIXED UNSTABLE
3	15	18	—	—	—	—	—	FIXED UNSTABLE
4	14	18	—	—	—	—	—	FIXED UNSTABLE
5	13	18	23	3466.67	24	4104.14	-637.47	FIXED
6	12	18	23	3466.67	24	3465.72	0.95	NESTED
7	11	18	23	3466.67	24	3348.28	118.38	NESTED
8	10	18	24	3466.67	24	3313.55	153.12	NESTED
9	9	18	23	3466.67	24	3301.41	165.25	NESTED
10	8	18	23	3466.67	24	3297.00	169.67	NESTED
11	7	18	23	3466.67	24	3295.43	171.24	NESTED
12	6	18	24	3466.67	24	3294.91	171.76	NESTED
13	5	18	24	3466.66	24	3294.83	171.83	NESTED
14	4	18	22	3466.65	24	3295.71	170.94	NESTED
15	3	18	24	3466.48	24	3303.72	162.76	NESTED
16	2	18	24	3465.00	24	3370.00	95.00	NESTED
17	1	18	13	3441.02	6	3685.36	-244.34	FIXED
Summary: NESTED wins: 11, FIXED-PARTITIONED wins: 2, Ties: 0								
Best FIXED-PARTITIONED advantage: $c_u = 5, c_n = 13$, advantage: 637.47								

The nested configuration won all 25 threshold comparisons with consistent advantages ranging from \$75.09 to \$153.12 per hour. In the bed combination analysis with total capacity $c = 18$, nested allocation won 11 configurations while fixed-partitioned won only 2, with the best fixed-partitioned advantage being \$637.47 per hour at $(c_u = 5, c_n = 13)$. This demonstrates that nested allocation still dominates in high-capacity systems with urgent-heavy patient mix, providing superior performance across most bed allocation strategies.

7. CONCLUSION

We propose and analyzes a simple, implementable occupancy-triggered redirection policy for managing ED congestion by routing selected low-acuity arrivals to alternative care when the department is crowded. Using a tractable two-class priority-queue framework, we characterize steady-state performance and determine an optimal redirection threshold under a long-run objective that balances revenue and congestion-related costs. Numerical experiments calibrated to representative rural and urban settings indicate that the optimal threshold is highly context dependent and that enabling alternative care yields consistent improvements relative to a no-redirection baseline across the parameter ranges tested. These improvements were up to 4.84% in rural settings and 5.90% in rural settings. Sensitivity analysis highlights the relative cost of urgent delay as a primary driver of both the optimal policy and the value of redirection. In addition, our capacity-allocation experiments suggest that allowing urgent patients to overflow into non-urgent capacity under preemptive priority often outperforms strict partitioning. Future work should incorporate richer operational features, including nonstationary arrivals, multiple acuity classes, and alternative-care capacity constraints, and should validate key economic and behavioral inputs using site-specific data.

REFERENCES

Alipour-Vaezi, M., Aghsami, A., and Jolai, F. (2022). Prioritizing and queueing the emergency departments' patients using a novel data-driven decision-making methodology, a real case study. *Expert Systems with Applications*, 195:116568.

Alnasser, S., Alharbi, M., AAlibrahim, A., Aal ibrahim, A., Kentab, O., Alassaf, W., and Aljähany, M. (2023). Analysis of emergency department use by non-urgent patients and their visit characteristics at an academic center. *International Journal of General Medicine*, 16:221–232.

American College of Emergency Physicians Task Force on Boarding (2008). Emergency department crowding: high-impact solutions. Acep task force report on boarding, American College of Emergency Physicians, Irving, TX.

Asplin, B., Magid, D., Rhodes, K., Solberg, L., Lurie, N., and Camargo, C. (2003). A conceptual model of emergency department crowding. *Annals of Emergency Medicine*, 42(2):173–180.

Association, A. H. (2025). Fast facts on u.s. hospitals, 2025. Technical report, American Hospital Association, Chicago, IL.

Cairns, C. and Kang, K. (2024). National hospital ambulatory medical care survey: 2022 emergency department summary tables. Technical report, National Center for Health Statistics, Hyattsville, MD.

Canellas, M., Michael, S., Kotkowski, K., and Reznek, M. (2023). Operations factors associated with emergency department length of stay: analysis of a national operations database. *Western Journal of Emergency Medicine*, 24(2):178–184. PMC10047726.

Centers for Medicare & Medicaid Services (2024). Medicare telehealth services list. Technical report, U.S. Department of Health and Human Services, Baltimore, MD.

Chrusciel, J., Fontaine, X., Devillard, A., Cordonnier, A., Kanagaratnam, L., Laplanche, D., and Sanchez, S. (2019). Impact of the implementation of a fast-track on emergency department length of stay and quality of care indicators in the champagne-ardenne region: a before-after study. *BMJ Open*, 9(6):e026200.

Considine, J., Kropman, M., Kelly, E., and Winter, C. (2008). Effect of emergency department fast track on emergency department length of stay: a case-control study. *Emergency Medicine Journal*, 25(12):815–819.

Cowling, T. and Majeed, A. (2013). Overuse of emergency departments. *JAMA*, 309(24):2549–2550.

Crawford, F. W., Ho, L. S. T., and Suchard, M. A. (2018). Computational methods for birth-death processes. *Wiley Interdisciplinary Reviews: Computational Statistics*, 10(2):e1423.

DeBehnke, D. and Decker, M. (2002). The effects of a physician-nurse patient care team on patient satisfaction in an academic ED. *American Journal of Emergency Medicine*, 20(4):267–270.

FairHealth Consumer (2024). Medical cost lookup tool. FairHealth Consumer, New York, NY.

Fermann, G. and Suyama, J. (2002). Point of care testing in the emergency department. *Journal of Emergency Medicine*, 22(4):393–404.

Ferrand, Y., Magazine, M., Rao, U., and Glass, T. (2018). Managing responsiveness in the emergency department: Comparing dynamic priority queue with fast track. *Journal of Operations Management*, 58-59(1):15–26.

Greenwood-Ericksen, M., Macy, M., Ham, J., Nypaver, M., Zochowski, M., and Kocher, K. (2019). Are rural and urban emergency departments equally prepared to reduce avoidable hospitalizations? *Western Journal of Emergency Medicine*, 20(3):477–484.

Grosse, S. D., Krueger, K. V., and Pike, J. (2019). Estimated annual and lifetime labor productivity in the United States, 2016: implications for economic evaluations. *Journal of Medical Economics*, 22(6):501–508.

Han, J., France, D., Levin, S., Jones, I., Storrow, A., and Aronsky, D. (2010). The effect of physician triage on emergency department length of stay. *Journal of Emergency Medicine*, 39(2):227–233.

Hou, J. and Zhao, X. (2020). Using a priority queuing approach to improve emergency department performance. *Journal of Management Analytics*, 7(1):28–43.

Jeyaraman, M., Alder, R., Copstein, L., Al-Yousif, N., Suss, R., Zarychanski, R., Doupe, M., Berthelot, S., Mireault, J., Tardif, P., Askin, N., Buchel, T., Rabbani, R., Beaudry, T., Hartwell, M., Shimmin, C., Edwards, J., Halas, G., Sevcik, W., Tricco, A., Chochinov, A., Rowe, B., and Abou-Setta, A. (2022). Impact of employing primary healthcare professionals in emergency department triage on patient flow outcomes: a systematic review and meta-analysis. *BMJ Open*, 12(4):e052850.

Jones, S., Moulton, C., Swift, S., Molyneux, P., Black, S., Mason, N., Oakley, R., and Mann, C. (2022). Association between delays to patient admission from the emergency department and all-cause 30-day mortality. *Emergency Medicine Journal*, 39(3):168–173.

Kamali, M., Tezcan, T., and Yildiz, O. (2019). When to use provider triage in emergency departments. *Management Science*, 65(3):1003–1019.

Kao, E. P. C. and Narayanan, K. S. (1991). Modeling a multiprocessor system with preemptive priorities. *Management Science*, 37(2):185–197.

Kennedy, M., Rosen, T., and Biese, K. (2025). Addressing the hospital boarding crisis in the us—time to act. *JAMA Internal Medicine*, 185(8):1038–1040.

Latouche, G. and Ramaswami, V. (1999). *Introduction to matrix analytic methods in stochastic modeling*. SIAM.

Liu, V., Fielding-Singh, V., Greene, J., Baker, J., Iwashyna, T., Bhattacharya, J., and Escobar, G. (2017). The timing of early antibiotics and hospital mortality in sepsis. *American Journal of Respiratory and Critical Care Medicine*, 196(7):856–863.

Mermiri, M., Mavrovounis, G., Chatzis, D., Mpoutsikos, I., Tsaroucha, A., Dova, M., Angelopoulou, Z., Ragias, D., Chalkias, A., and Pantazopoulos, I. (2021). Critical emergency medicine and the resuscitative care unit. *Acute and Critical Care*, 36(1):22–28.

Morley, C., Unwin, M., Peterson, G., Stankovich, J., and Kinsman, L. (2018). Emergency department crowding: A systematic review of causes, consequences and solutions. *PLoS ONE*, 13(8):e0203316.

Nambiar, S., Mayorga, M., and Liu, Y. (2023). Routing and staffing in emergency departments: A multiclass queueing model with workload dependent service times. *IIE Transactions on Healthcare Systems Engineering*, 13(1):46–61.

Neuts, M. (1994). *Matrix-geometric solutions in stochastic models: an algorithmic approach*. Courier Corporation.

Nyce, A., Gandhi, S., Freeze, B., Bosire, J., Ricca, T., Kupersmith, E., Mazzarelli, A., and Rachoin, J. (2021). Association of emergency department waiting times with patient experience in admitted and discharged patients. *Journal of Patient Experience*, 8:23743735211011404.

Parnass, G., Levzion-Korach, O., Peres, R., and Assaf, M. (2023). Estimating emergency department crowding with stochastic population models. *PLoS ONE*, 18(12):e0295130.

Patel, M. D., Lin, P., Cheng, Q., Argon, N. T., Evans, C. S., Linthicum, B., Liu, Y., Mehrotra, A., Murphy, L., and Ziya, S. (2024). Patient sex, racial and ethnic disparities in emergency department triage: a multi-site retrospective study. *American Journal of Emergency Medicine*, 76:29–35.

Patel, P. and Vinson, D. (2005). Team assignment system: expediting emergency department care. *Annals of Emergency Medicine*, 46(6):499–506.

Phillips, K., Knowlton, M., and Riseden, J. (2022). Emergency department nursing burnout and resilience. *Advanced Emergency Nursing Journal*, 44(1):54–62.

Powell, E., Khare, R., Venkatesh, A., Van Roo, B., Adams, J., and Reinhardt, G. (2012). The relationship between inpatient discharge timing and emergency department boarding. *The Journal of Emergency Medicine*, 42(2):186–196.

Rathlev, N., Visintainer, P., Schmidt, J., Hettler, J., Albert, V., and Li, H. (2020). Patient characteristics and clinical process predictors of patients leaving without being seen from the emergency department. *Western Journal of Emergency Medicine*, 21(5):1218–1226.

Rooney, K. and Schilling, U. (2014). Point-of-care testing in the overcrowded emergency department—can it make a difference? *Critical Care*, 18(6):692.

Saghafian, S., Austin, G., and Traub, S. (2015). Operations research/management contributions to emergency department patient flow optimization: review and research prospects. *IIE Transactions on Healthcare Systems Engineering*, 5(2):101–123.

Sartini, M., Carbone, A., Demartini, A., Giribone, L., Oliva, M., Spagnolo, A., Cremonesi, P., Canale, F., and Cristina, M. (2022). Overcrowding in emergency department: Causes, consequences, and solutions—a narrative review. *Healthcare*, 10(9):1625.

Savioli, G., Ceresa, I., Gri, N., Bavestrello Piccini, G., Longhitano, Y., Zanza, C., Piccioni, A., Esposito, C., Ricevuti, G., and Bressan, M. (2022). Emergency department overcrowding: understanding the factors to find corresponding solutions. *Journal of Personalized Medicine*, 12(2):279.

Scott, A., Sanders, S., Atkins, T., van der Merwe, M., Sunner, C., Clark, J., and Glasziou, P. (2025). The impact of telehealth care on escalation to emergency care: A systematic review and meta-analysis. *Journal of Telemedicine and Telecare*, 31(8):1059–1077.

Shortle, J. F., Thompson, J. M., Gross, D., and Harris, C. M. (2018). *Fundamentals of queueing theory*. John Wiley & Sons, 5th edition.

Sun, S., Lu, S., and Rui, H. (2020). Does telemedicine reduce emergency room congestion? evidence from new york state. *Information Systems Research*, 31(3):972–986.

Tsou, C., Robinson, S., Boyd, J., Jamieson, A., Blakeman, R., Yeung, J., McDonnell, J., Waters, S., Bosich, K., and Hendrie, D. (2021). Effectiveness of telehealth in rural and remote emergency departments: Systematic review. *Journal of Medical Internet Research*, 23(11):e30632.

Weinick, R. M., Burns, R. M., and Mehrotra, A. (2010). Many emergency department visits could be managed at urgent care centers and retail clinics. *Health Affairs*, 29(9):1630–1636.

Yun, B., Singh, M., Reznik, M., Buehler, G., Wolf, S., Vogel, L., Ho, A., Pino, E., Ellis, L., and Arbelaez, C. (2025). Strengthening essential emergency departments: Transforming the safety net. *Health Affairs Scholar*, 3(3):qxaf044.

Zayas-Caban, G., Xie, J., Green, L., and Lewis, M. (2019). Policies for physician allocation to triage and treatment in emergency departments. *IISE Transactions on Healthcare Systems Engineering*, 9(4):342–356.

APPENDIX A. ADDITIONAL PROOFS

Backward Recursive Formula:

$$\mathbf{x}_h U_{i-1} B + \mathbf{x}_h U_i A_i + \mathbf{x}_h U_{i+1} C_{i+1} = \mathbf{0}.$$

Since \mathbf{x}_h has strictly positive entries, solving for U_{i-1} we get

$$U_{i-1} = -(U_i A_i + U_{i+1} C_{i+1}) B^{-1} = -\frac{1}{\lambda_u} (U_i A_i + U_{i+1} C_{i+1}),$$

where we have used the fact that $B^{-1} = \frac{1}{\lambda_u} I_k$. Substituting C_{i+1} :

$$U_{i-1} = -\frac{1}{\lambda_u} (U_i A_i + (\mu_u \min\{i+1, c\}) U_{i+1})$$

Now, we convert (A) using the backward indexing notation U_{h-i} . That is, for levels $i = 2, \dots, h$:

$$U_{h-i} = -\frac{1}{\lambda_u} (U_{h-i+1} A_{h-i+1} + \mu_u \min\{h-i+2, c\} U_{h-i+2},)$$

From the equation for level h in (4.1.3) we have similarly

$$\mathbf{x}_h (U_{h-1} B + A + \rho_u C) = \mathbf{0}$$

Therefore,

$$U_{h-1} = -\frac{1}{\lambda_u} (A + \rho_u C)$$

Substituting the value of ρ_u from (7) and C from 4.1.1.(ii) we get

$$U_{h-1} = -\frac{1}{\lambda_u} \left(A + \frac{\lambda_u}{\mu_u c} \cdot \mu_u c \right) = -\frac{1}{\lambda_u} (A + \lambda_u I_k) = -\frac{1}{\lambda_u} A - I_k.$$

Our complete recursive approach can now be summarized below:

$$\begin{aligned} U_h &= I \\ U_{h-1} &= -\frac{1}{\lambda_u} A - I \\ U_{h-i} &= -\frac{1}{\lambda_u} (U_{h-i+1} A_{h-i+1} + \mu_u \min\{h-i+2, c\} U_{h-i+2}) \end{aligned}$$

We need to find \mathbf{x}_h in order to get the steady state distribution from the backward recursive approach. From (4.1.3) and using $\mathbf{x}_i = \mathbf{x}_h U_i$

$$\mathbf{x}_h (U_0 A_0 + U_1 C_1) = \mathbf{0}$$

Furthermore notice

$$\sum_{i=0}^{h-1} \mathbf{x}_i \mathbf{e} + \sum_{i=h}^{\infty} \mathbf{x}_i \mathbf{e} = 1,$$

For $i = 0, \dots, h-1$:

$$\sum_{i=0}^{h-1} \mathbf{x}_i \mathbf{e} = \sum_{i=0}^{h-1} (\mathbf{x}_h U_i) \mathbf{e} = \mathbf{x}_h \sum_{i=0}^{h-1} U_i \mathbf{e} = \mathbf{x}_h \left(\sum_{i=0}^{h-1} U_i \right) \mathbf{e}$$

Now using (7)

$$\sum_{i=h}^{\infty} \mathbf{x}_i \mathbf{e} = \sum_{n=0}^{\infty} (\mathbf{x}_h \rho_u^n) \mathbf{e} = (1 - \rho_u)^{-1} \mathbf{x}_h \cdot \mathbf{e}.$$

Substituting (A) and (A) to (A) we get

$$1 = \mathbf{x}_h \left(\sum_{i=0}^{h-1} U_i \right) \mathbf{e} + (1 - \rho_u)^{-1} \mathbf{x}_h \cdot \mathbf{e} = \mathbf{x}_h \left[\sum_{i=0}^{h-1} U_i + (1 - \rho_u)^{-1} I \right] \mathbf{e}$$

Therefore,

$$\mathbf{x}_h \left[\sum_{i=0}^{h-1} U_i + (1 - \rho_u)^{-1} \right] \mathbf{e} = 1.$$

APPENDIX B. ALGORITHMS

B.0.1. *QBD Algorithm.* The following algorithm outlines the steps to determine the steady-state and evaluate queue metrics.

Algorithm 1 QBD Steady-State Solution for Emergency Department Model - Part 1

- 1: **Input:** $\lambda, p_u, \mu_u, \mu_n, c_u, c_n, k, \theta, p_{\text{accept}}$
- 2: **Output:** Steady-state probabilities $\pi(i, j)$ and performance measures
- 3: **Step 1: Initialize Parameters**
- 4: $p_n \leftarrow 1 - p_u, \lambda_u \leftarrow p_u \cdot \lambda, c \leftarrow c_u + c_n$
- 5: $h \leftarrow \max(k, c), \rho_u \leftarrow \frac{p_u \lambda}{\mu_u c}$
- 6: **Step 2: Verify Stability**
- 7: **if** $\rho_u \geq 1$ **then**
- 8: **return** "System is unstable"
- 9: **end if**
- 10: **Step 3: Define System Functions**

$$\alpha(i, j) = \begin{cases} 1 & \text{if } i + j < \theta \\ 1 - p_{\text{accept}} & \text{if } \theta \leq i + j < k \\ 0 & \text{if } i + j \geq k \end{cases}$$

- 11: $s_u(i) = \min\{c, i\}, s_n(i, j) = \min\{\max\{0, c - i\}, j, c_n\}$

- 12: **Step 4: Construct QBD Matrices**

- 13: **for** $i = 0$ to $h - 1$ **do**
- 14: $B \leftarrow p_u \lambda I_k$
- 15: $\mathbf{C}_i \leftarrow \mu_u \min\{i, c\} \cdot I_k$
- 16: **for** $j = 0$ to $k - 1$ **do**
- 17: **if** $j < k - 1$ **then**
- 18: $d_{j, j+1}^{(i)} \leftarrow \lambda_n \alpha(i, j)$
- 19: **end if**
- 20: **if** $j > 0$ **then**

```

21:    $a_{j,j-1}^{(i)} \leftarrow \mu_n s_n(i, j)$ 
22:   end if
23:    $a_{j,j}^{(i)} \leftarrow -(\lambda_u + \lambda_n \alpha(i, j) + \mu_u s_u(i) + \mu_n s_n(i, j))$ 
24: end for
25: end for
26:  $A \leftarrow A_h, \mathbf{C} \leftarrow \mu_u c \cdot I_k$ 
27: Step 5: Backward Recursive Computation
28:  $U_h \leftarrow I_k, U_{h-1} \leftarrow -\frac{1}{p_u \lambda} A - I_k$ 
29: for  $i = 2$  to  $h$  do
30:    $U_{h-i} \leftarrow -\frac{1}{p_u \lambda} (U_{h-i+1} A_{h-i+1} + \mu_u \min\{h - i + 2, c\} U_{h-i+2})$ 
31: end for

```

Algorithm 2 QBD Steady-State Solution for Emergency Department Model - Part 236: **Step 6: Solve for \mathbf{x}_h**

37: Solve

$$\mathbf{x}_h (U_0 A_0 + U_1 C_1) = \mathbf{0},$$

38: and use

$$\mathbf{x}_h \left[\sum_{i=0}^{h-1} U_i + \left(1 - \frac{p_u \lambda}{\mu_u (c_u + c_n)} \right)^{-1} I_k \right] \mathbf{e} = 1$$

as the last row of the above system to determine \mathbf{x}_h^* .39: **Step 7: Compute Complete Steady-State Distribution**40: **for** $i = 0$ to $h - 1$ **do**41: $\mathbf{x}_i \leftarrow \mathbf{x}_h U_i$ 42: **end for**43: **for** $i = h$ to ∞ **do**44: $\mathbf{x}_i \leftarrow \mathbf{x}_h \rho_u^{i-h}$ 45: **end for**46: **Step 8: Extract Individual State Probabilities**47: **for** $i = 0$ to ∞ **do**48: **for** $j = 0$ to $k - 1$ **do**49: $\pi(i, j) \leftarrow \mathbf{x}_i[j]$ { j -th element of vector \mathbf{x}_i }50: **end for**51: **end for**52: **Step 9: Compute Performance Measures**53: $E[N] \leftarrow \sum_{i=0}^{\infty} \sum_{j=0}^{k-1} (i + j) \pi(i, j)$ 54: $E[N_n] \leftarrow \sum_{i=0}^{\infty} \sum_{j=0}^{k-1} j \cdot \pi(i, j)$ 55: $\lambda_n^{eff} \leftarrow \sum_{i=0}^{\infty} \sum_{j=0}^{k-1} \lambda_n \alpha(i, j) \pi(i, j)$ 56: **Step 10: Calculate Waiting Time for Non-Urgent Patients Using Little's Law**57: $E[W_n] \leftarrow \frac{E[N_n]}{\lambda_n^{eff}}$ 58: where λ_n^{eff} shows the effective rate of non-urgent patients entering the ED.

 59: **return** $\{\pi(i, j), E[N], E[N_n], E[W_n]\}$

Algorithm 3 Direct Capacity Optimization for Emergency Department

Require: Total capacity c , system parameters

Ensure: Optimal capacity allocation (c_u^*, c_n^*)

 1: Initialize best_objective = $-\infty$, $(c_u^*, c_n^*) = (1, c - 1)$
 2: **for** $c_u = 1$ **to** $c - 1$ **do**
 3: Set $c_n = c - c_u$
 4: Find optimal threshold: $\theta^* = \arg \max_{\theta} Z(c_u, c_n, \theta)$
 5: Solve QBD system with (c_u, c_n, θ^*)
 6: Calculate objective: $Z(c_u, c_n, \theta^*)$
 7: **if** $Z(c_u, c_n, \theta^*) > \text{best_objective}$ **then**
 8: best_objective = $Z(c_u, c_n, \theta^*)$
 9: $(c_u^*, c_n^*) = (c_u, c_n)$
 10: **end if**
 11: **end for**

 12: **Output:** Optimal capacity allocation

APPENDIX C. PARAMETER DERIVATION

(i) **Arrival Rate.** The arrival rate λ is calculated from NHAMCS 2022 national ED visit data by patient residence (Cairns and Kang, 2024) and AHA hospital counts (Association, 2025). Urban visits (123.246 million visits/3,316 hospitals) and rural visits (27.548 million visits/1,796 hospitals) is converted to hourly rates.

(ii) **Urgent Patient Proportion.** The proportion of ED patients triaged as urgent (p_u) is calculated using triage severity levels. For urban hospitals, we use the Emergency Severity Index (ESI) from Patel et al. (2024), where ESI 1 (2%), ESI 2 (22%), and ESI 3 (61%) yields $p_u = 0.85$. For rural hospitals, since literature suggests that the proportion of non-urgent patients in rural ED is higher than Urban ED, we use findings from Alnasser et al. (2023), where 61.4% of ED visits were less-urgent or non-urgent, yielding approximately $p_u = 0.39$.

(iii) **Service Rates.** The service rates μ_u, μ_n are derived from national ED operations benchmarks (Canellas et al., 2023) showing median length of stay for admitted patients (289 minutes) and discharged patients (147 minutes), adjusted for door-to-clinician time (16 minutes) from NHAMCS 2022 (Cairns and Kang, 2024). Service rates are calculated using the exponential distribution relationship $\mu = \ln(2)/\text{median}$, yielding $\mu_u = 0.15$ and $\mu_n = 0.32$ patients per hour.

(iv) **Bed Capacity.** The total bed capacity c is derived from (Greenwood-Ericksen et al., 2019, Table 1), which reports median emergency department bed counts by hospital type. Rural hospitals have a median of approximately 9 beds while urban hospitals have a median of 34 beds.

(v) **Bed Allocation Ratio.** Based on empirical data from Stony Brook University Medical Center (Mermiri et al., 2021), which operates a 22-bed resuscitative emergency department ICU (RED-ICU) with 8 beds designated as an Acute Critical Care Subunit for the highest acuity patients, we obtain a bed allocation ratio of $c_u/c = 8/22 = 0.36 \approx 0.4$ for urgent bed allocation.

(vi) **Alternative Care Acceptance Rate.** The probability of accepting alternative care or alternative care offers (p_a) is derived from [Weinick et al. \(2010\)](#), which found that 52% of eligible non-urgent ED patients accepted referral to alternative option when offered after triage.

(vii) **Revenue Parameters.** ED revenue parameters are derived from FairHealth Consumer medical cost data ([FairHealth Consumer, 2024](#)) for ZIP code 16803, combining facility and physician costs for both in-network and out-of-network pricing across CPT codes 99281-99285. Non-urgent ED revenue ($r_n^{ED} = \$675.50$) represents the simple average of CPT codes 99281 (\$554) and 99282 (\$797). Urgent ED revenue ($r_u^{ED} = \$2,221.00$) represents the average of CPT codes 99283 (\$1,483), 99284 (\$2,356), and 99285 (\$2,824). Each code average combines facility costs and primary medical procedure costs for both in-network and out-of-network pricing, reflecting the mixed payer composition typical of emergency departments. Telemedicine revenue ($r^{Tele} = \$116.50$) is derived from FairHealth Consumer medical cost data ([FairHealth Consumer, 2024](#)) for CPT code Q3014 tele-health services, representing the average of out-of-network price (\$154) and in-network price (\$79). Alternative option revenue ($r^{Alt} = \$436.00$) is derived from the same resource and methodology for hospital outpatient/clinic visits code G0463, yielding \$436.00.

(viii) **Balking Cost.** We represent balking cost c^b as expected revenue loss when patients balk or do not enter the system. We calculate this for two scenarios: With respect to alternative care, $c^b = (1 - p_a) \cdot r_n^{ED} + p_a \cdot r^{Tele}$ yielding $c^b = 0.48 \times 675.50 + 0.52 \times 116.50 = \384.82 . With respect to alternative care, $c^b = (1 - p_a) \cdot r_n^{ED} + p_a \cdot r^{Alt}$ yielding $c^b = 0.48 \times 675.50 + 0.52 \times 436.00 = \550.96 .

(ix) **Waiting Costs (Non-urgent):** Based on empirical LWBS (Left Without Being Seen) behavior from [Rathlev et al. \(2020\)](#), showing baseline LWBS rate of 1.41% for patients seen within 30 minutes, increasing to 3.25%, 7.00%, 10.02%, and 14.46% for successive 30-minute intervals. The incremental increases per 30-minute period are: 3.75% (30-60 min), 3.02% (60-90 min), and 4.44% (90-120 min). The average linear growth rate is calculated as $(3.75 + 3.02 + 4.44)/3 = 11.21/3 \approx 3.74\%$ per 30-minute period. This yields the model $c_n^w = \frac{(0.014 + 0.0374 \times 2 \times \text{LOS}) \times r_n^{ED}}{\text{LOS}}$, where the LWBS rate increases linearly with waiting time. Mean non-urgent LOS of 3.53 hours is calculated from the exponential distribution median relationship: Mean LOS = Median / $\ln(2) = 147 \text{ min} / 0.693 = 212.08 \text{ min} = 3.53 \text{ hours}$, using median LOS for discharged patients ([Canellas et al., 2023](#)). With $r_n^{ED} = \$675.50$ and substituting values: $c_n^w = \frac{(0.014 + 0.0748 \times 3.53) \times 675.50}{3.53} = 53.21\text{\$ per hour}$.

(x) **Waiting Costs (Urgent):** Average urgent patient age of 47.0 years is calculated from high-priority patients (triage Levels 1, 2, and 3: immediate, emergent, and urgent) in the 2022 National Hospital Ambulatory Medical Care Survey ([Cairns and Kang, 2024, Table 6](#)) using weighted averages: urgent visits by age group are Under 15: $26,463 \times (0.2\% + 4.2\% + 22.3\%) = 7,066$ visits; 15-24: $20,675 \times (0.7\% + 6.9\% + 29.7\%) = 7,712$ visits; 25-44: $39,547 \times (0.8\% + 8.7\% + 34.5\%) = 17,401$ visits; 45-64: $35,778 \times (1.2\% + 12.9\% + 35.1\%) = 17,603$ visits; 65+: $32,935 \times (1.8\% + 15.4\% + 40.3\%) = 18,938$ visits, yielding $\frac{\sum(\text{urgent visits}_i \times \text{midpoint age}_i)}{\sum(\text{urgent visits}_i)} = \frac{7,066 \times 7.5 + 7,712 \times 19.5 + 17,401 \times 34.5 + 17,603 \times 54.5 + 18,938 \times 77.5}{68,720} = 47.0$ years. Based on sepsis mortality studies ([Liu et al., 2017](#)), analysis shows 0.4% mortality increase per hour of treatment delay. The present value of remaining lifetime productivity at age 47 is calculated by linear interpolation between ages 40 and 50 from productivity estimates ([Grosse et al., 2019](#)) using 1% annual productivity growth and 3% discount rate: $\frac{(50-47) \times \$1,769,257 + (47-40) \times \$1,217,322}{50-40} = \$1,382,902.5$. The

urgent waiting cost model is: urgent waiting cost per hour = mortality increase per hour \times present value of lifetime productivity, yielding $c_u^w = 0.004 \times \$1,382,902.5 = \$5,531.61$ per hour.

APPENDIX D. ADDITIONAL PROPORTIONAL PLOTS

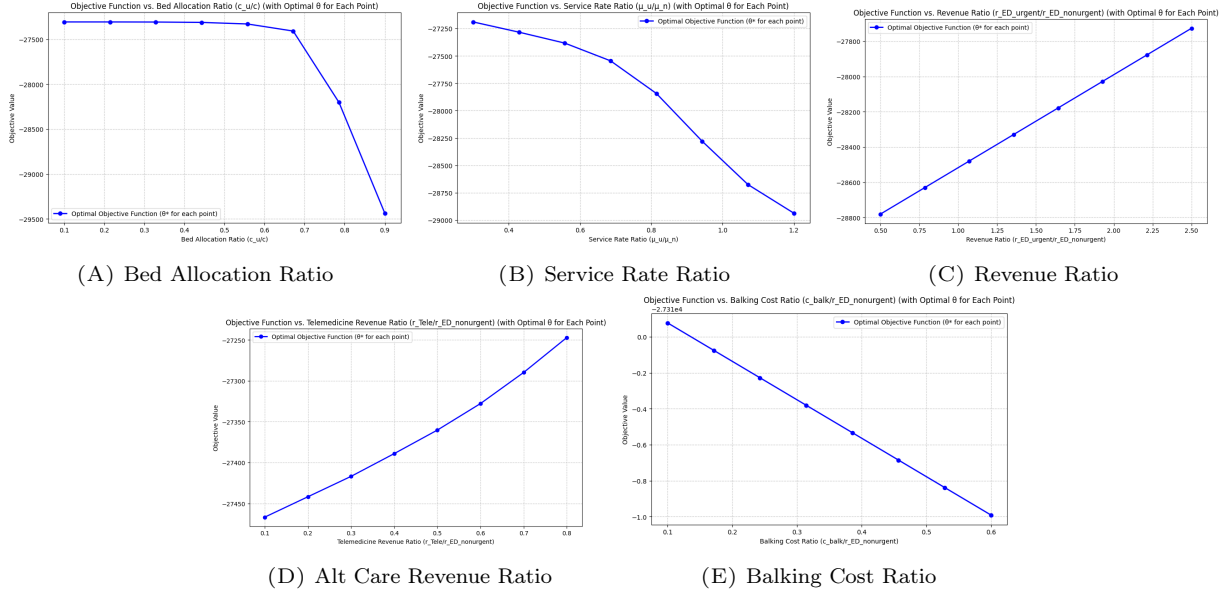


FIGURE 13. Baseline Case Analysis: Rural Alternative Care-enabled ED

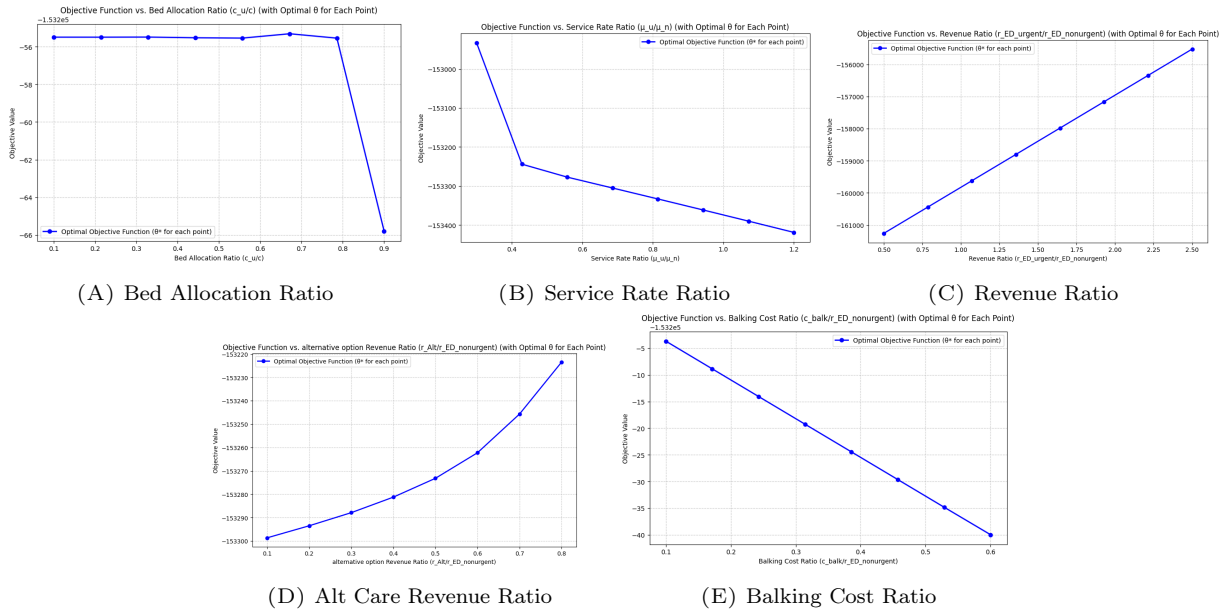


FIGURE 14. Baseline Case Analysis: Urban Alternative Care-enabled ED